The critical role of infectious disease in compensatory population growth in response to culling

The critical role of infectious disease in compensatory population growth in response to culling

Eleanor Tanner[1,*]

Andy White[1]

Peter, W.W. Lurz[2]

Christian Gortázar[3]

Iratxe Díez-Delgado[3]

Mike Boots[4,5]

1. Maxwell Institute for Mathematical Sciences, Department of Mathematics, Heriot-Watt University, Edinburgh, EH14 4AS, UK.;

2. Lurzengasse 3, D-97236 Randersacker, Germany.;

3. SaBio, Instituto de Investigación en Recursos Cinegéticos IREC (CSIC-UCLM), Ciudad Real, Spain;

4. Department of Integrative Biology, University of California, Berkeley, CA 94720, USA;

5. Biosciences, College of Life and Environmental Sciences, University of Exeter, Cornwall Campus, Treliever Road, Penryn, Cornwall, TR10 9EZ, UK.

∗ Corresponding author; e-mail: ent1@hw.ac.uk.

Manuscript elements: Figure 1, figure 2, figure 3, figure 4, figure 5, and figure 6, online appendix A (including figure A1, figure A2, figure A3, figure A4, figure A5, figure A6, figure A7, figure A8, figure A9 and figure A10). Figure 1, figure 2, figure 3, figure 4, figure 5, and figure 6 are to print in color.

Keywords: Culling, disease dynamics, virulence, immunity, compensatory growth, hydra effect.

Manuscript type: Article.

Prepared using the suggested LaTeX template for *Am. Nat.*

Abstract

Despite the ubiquity of disease in nature, the role that disease dynamics play in the compensatory growth response to harvesting has been ignored. We use a mathematical approach to show that harvesting can lead to compensatory growth due to a release from disease-induced mortality. Our findings imply that culling in systems that harbor virulent parasites can reduce disease prevalence and increase population density. Our models predict that this compensation occurs for a broad range of infectious disease characteristics unless disease induces long-lasting immunity in hosts. Our key insight is that a population can be regulated at a similar density by disease or at reduced prevalence by a combination of culling and disease. We illustrate our predictions with a system-specific model representing wild boar tuberculosis infection, parameterized for central Spain, and find significant compensation to culling. Given that few wildlife diseases are likely to induce long-lived immunity, populations with virulent diseases may often be resilient to harvesting.

Introduction

It is well known that harvesting may be compensated by an increased growth rate at lower density (Abrams 2009). This phenomenon of compensatory growth in response to culling was first modelled by Ricker (1954) who showed that for moderate harvesting levels the population can stabilize to a level that exceeds the density in the absence of harvesting. Despite the ubiquity of infectious disease in nature, little work has considered the impact of harvesting and culling in populations with virulent infectious disease and the compensatory potential of changes to disease dynamics. Since culling affects the disease dynamics there is considerable potential to generate feedbacks on host population dynamics. Moreover, as culling is also used as a management strategy to control emergent wildlife diseases, it is vital to understand the interplay between culling, disease and population dynamics (Barlow 1996; Woodroffe 1999). In this study we develop mathematical models to examine the impact of culling in systems that support endemic diseases and for the first time detail how culling can lead to compensatory growth due to a reduction in disease-induced mortality.

It is difficult to gather field data to test theories about the population-level implications of complex disease dynamics (Abrams 2009; McCallum 2016). Mathematical models are therefore important tools for explaining the impact of culling and harvesting in systems with endemic parasites. There is an extensive modelling literature focussed on the control of disease through culling, for example chronic wasting disease in deer in North America (Potapov et al. 2012; Storm et al. 2013; Uehlinger et al. 2016; Wasserberg et al. 2009); acutely virulent classical swine fever in wild boar (Bolzoni et al. 2007; Choisy and Rohani 2006; Cowled et al. 2012); and lethal facial tumour disease in Tasmanian devils (Beeton and McCallum 2011). While these studies recognize that culling in systems with endemic disease can induce compensation through demographic processes, they have not examined how culling may lead to compensatory effects that arise directly from changes in disease dynamics.

The limited work that has examined the effect of culling on disease dynamics has shown that

culling may increase prevalence due to a decrease in long-lasting immunity or vaccine coverage (Bolzoni et al. 2007; Choisy and Rohani 2006; Potapov et al. 2012), with Potapov et al. (2012) showing that prevalence can decrease in a system with no immunity. However, these studies have not examined compensatory effects due to disease and have only considered a limited range of disease characteristics. Here, we model in general the impacts of culling and harvesting in systems that support a wide range of endemic diseases. A novel aspect of our study is that we isolate the compensatory effects following culling due to changes in the disease dynamics resulting from a population level release from disease-induced mortality. This facet is vital if we are to understand the response of harvesting in managed and natural systems that harbor virulent parasites. We show that significant host compensation occurs in response to culling for infections that do not cause long-lasting immunity and therefore such host populations can be more sustainable. However, when there is long-lasting immunity the disease can decrease the population's resilience to harvesting and increase its extinction risk when culling is used to manage a disease. We develop a system-specific model of *Sus scrofa* (wild boar) tuberculosis interactions that illustrates our predictions in a specific disease context. Our work highlights the importance of understanding the nature of immunity to infectious disease for sustainable harvesting of populations and the management of disease through culling.

Methods

We examine a classical compartmental SIRS model of disease (Anderson and May 1979; Keeling and Rohani 2008) that considers a total population (N) split into separate classes representing different disease stages: the class of susceptibles (S), of infecteds (I) and of recovereds/immunes (R), such that the total population density is $N = S + I + R$. In this model all classes reproduce and all newborns are susceptible. The maximum per capita birth rate b decreases with increasing density through parameter q and all population classes incur natural death at rate d. A susceptible individual becomes infected with transmission rate function $\theta(I, N)$ which can represent

density-dependent (DD) or frequency-dependent (FD) disease transmission (equations (4) and (5) respectively). Infected individuals incur additional disease-induced mortality (virulence) at rate α and can recover from infection to become immune from the disease at rate γ. Immunity can be lost causing recovereds to become susceptible again at rate η. This model is represented with the following system of ordinary differential equations:

$$\frac{\mathrm{d}S}{\mathrm{d}t} = bN(1-qN) - dS - \theta(I,N)S + \eta R \tag{1}$$

$$\frac{\mathrm{d}I}{\mathrm{d}t} = \theta(I,N)S - dI - \alpha I - \gamma I \tag{2}$$

$$\frac{\mathrm{d}R}{\mathrm{d}t} = \gamma I - dR - \eta R. \tag{3}$$

A strength of our model is that it can be adapted to represent a range of classical infection frameworks: SI by setting $\gamma = 0$; SIR by setting $\gamma > 0$ and $\eta = 0$; and SIRS with both $\gamma > 0$ and $\eta > 0$. The system is normalized to a common endemic steady state $N = N_e$ ($S = S_e$, $I = I_e$, $R = R_e$ and we choose $N_e = 1$ without loss of generality) when the initial prevalence prior to culling is $p_i\,(= I_e/N_e)$, see online appendix A, section A1 for further details. The endemic transmission functions are defined as follows:

$$\text{DD transmission}: \quad \theta(I,N) = \frac{(d+\alpha+\gamma)}{N_e\left(1 - p_i\left(\frac{\gamma}{d+\eta}+1\right)\right)} I \tag{4}$$

$$\text{FD transmission}: \quad \theta(I,N) = \frac{(d+\alpha+\gamma)}{\left(1 - p_i\left(\frac{\gamma}{d+\eta}+1\right)\right)} \frac{I}{N}. \tag{5}$$

Under this set-up we can compare results for systems that have the same initial density and initial level of prevalence prior to culling.

We examine the dynamics exhibited by the model (equations (1-3)) when the population is subject to indiscriminate culling (i.e. an equal proportion is removed from each class in the model). We implement the culling regime as a discrete event that removes a fixed percentage of the population with continuous population regrowth between each cull event. Culling occurs at unit time intervals leading to $1/d$ culls during the average lifetime of an individual in the absence of the disease. We run the culling regime for 30 consecutive periods of instantaneous

cull followed by regrowth and examine the effect on the disease prevalence and the population density both during and at the end of this culling regime. In particular, we define the 'resultant density' as the population density at the end of the 30 consecutive cull and subsequent regrowth events. Note, our results are qualitatively similar if we assume culling occurs continuously rather than as a discrete event (see below and online appendix A, section A2). Our results are produced numerically using MATLAB ODE solvers.

In addition to assessing the impact of culling on the dynamics in the full model (equations (1-3)) we also develop a model whose dynamics can respond to culling through demographic effects only:

$$\frac{\mathrm{d}N}{\mathrm{d}t} = bN(1-qN) - dN - \alpha p_i N. \tag{6}$$

This 'demographic effects only model' has the equivalent level of mortality to the full model (equations (1-3)) at the endemic steady state but it cannot respond to changes in disease prevalence and therefore allows us to isolate the importance of changes to the disease dynamics as a result of culling. The parameters b, d, q and α are the same as in the full model (equations (1-3)), p_i is the initial prevalence in the full model (which is constant in this model) and therefore prior to culling both models have the same steady state density $N = N_e$. Importantly, the density-dependent per capita birth rate, $b(1-qN)$, has an identical response in both models and therefore any changes to the density in response to culling lead to the same change in the per capita birth rate.

We now note that the dynamics of the total density in the full model (found by summing equations (1-3)) can be written as:

$$\frac{\mathrm{d}N}{\mathrm{d}t} = bN(1-qN) - dN - \alpha \frac{I}{N} N. \tag{7}$$

Prior to culling the level of mortality is the same, since $p_i = Ie/Ne$. Critically, however, culling can lead to a change in the disease dynamics and therefore a change in disease prevalence I/N. This can lead to a change in the rate of mortality in the full model but not in the demographic effects model since p_i does not change. A comparison of the full model and the demographic

effects only model therefore allows us to determine the importance of changes due to the disease dynamics as a result of culling.

We also develop a 'disease effects only' model which has the same disease dynamics as the full model (equations (1-3)) but has a fixed per capita birth rate $b(1 - qN_e)$ and therefore dynamic population density does not affect the rate of reproduction. This model is the same as equations (1-3) except for equation (1) which is modified as follows:

$$\frac{\mathrm{d}S}{\mathrm{d}t} = bN(1 - qN_e) - dS - \theta(I, N)S + \eta R. \tag{8}$$

For DD transmission the disease effects only model has the same endemic steady state, N_e, as the full model and therefore we can compare results between the disease effects only model and the full model to understand the contribution of demographic effects on compensatory growth. However, for FD transmission, the disease effects only model does not have a comparable non-zero endemic steady state so this comparison is not valid. (In a similar manner a model that cannot respond through disease or demographic effects cannot be compared to the full model, as culling would lead to population extinction.)

Analysing the results for these models allows us to compare the compensatory growth following culling that is due to: both demographic and disease effects (represented by the full model, equations (1-3)); demographic effects only (represented by equations (6)); and disease effects only (represented by equation (8)). The difference between the population densities in response to culling in these models allows us to partition compensatory growth due to disease dynamics only, namely a population level release from disease-induced mortality, and compensatory growth due to demographic effects. In this study we wish to understand the importance of compensatory growth due to a release from disease-induced mortality in response to culling for a range of key infection representations.

We examine the behaviour of the model, equations (1-3), with DD and FD transmission for a SI framework (no recovery from infection) and for a SIR framework which represents life-long immunity to infection. Later we consider a SIRS framework in which immunity can wane over

time; targeted culling on infected individuals only; and density-dependent mortality in addition to density-dependent reproduction. In addition to assessing the impact of culling in systems with classical modes of directly transmitted infection (DD and FD) we have also undertaken our analysis for systems with environmental, free-living (FL) transmission (Anderson and May 1981). The results for FL transmission are qualitatively similar to those with DD transmission and general results are detailed in online appendix A, section A3. To emphasize the breadth of our findings the results for systems with FL transmission are highlighted in the case study on the impact of culling on wild boar tuberculosis interactions.

Results

The effects of culling in populations with virulent infection and no recovery

Figure 1a(i-ii) shows that culling does not greatly decrease population density in systems with DD transmission in the absence of recovery. Indeed, after the initial culling events, the resultant density immediately prior to the next cull reaches a level exceeding the initial density $N_e = 1$. Moreover, the density can reach higher levels under a 25% cull than under a 10% cull. Here, culling leads to compensatory (even over-compensatory) growth as a result of changes to the disease dynamics. In particular, there is a reduction in the infected density and increase in susceptible density (figure 1a(i-ii)) and therefore, as the total population density is not diminished, there is a reduction in disease prevalence (figure 1c(i-ii)) which reduces the level of disease-induced mortality suffered by the population. The reduction in prevalence is greater under the higher level of culling and so the compensatory growth due to infection processes is greater under higher culling. Under FD transmission the total population size increases less in response to culling (figure 1b(i-ii)) but again there is a reduction in the infected density and increase in susceptible density that mitigates some of the mortality due to culling. The reduction in disease prevalence due to culling is smaller under FD compared to DD transmission (figure 1c(i-ii)), which may explain the lower compensatory response.

To understand these findings more clearly we examine the results for a 25% cull in population phase space (figure 2i) and in terms of changes in the force of infection (figure 2ii). Under DD transmission the population response following the initial culls is an increase in susceptibles but a decrease in infectives (figure 2a(i)), since culling reduces the force of infection (figure 2a(ii)). Eventually, the density prior to the next cull stabilizes, with an increased density of susceptibles, a decreased level of infecteds and a decreased force of infection. In this way the increased mortality due to culling is compensated by population level decreases in mortality due to the disease. Under FD transmission the population response following initial culls is an increase in susceptible and infected density (figure 2b(i)). In particular, culling does not reduce the force of infection under FD transmission (figure 2b(ii)) as much, particularly in the initial culling events. The resultant population therefore supports a higher level of infecteds compared to DD transmission, and therefore while the compensatory effects due to reduced population level disease-induced mortality are still significant they are smaller under FD transmission.

The compensatory population growth in response to culling can result from two mechanisms: a reduction in the impact of density dependence on reproduction; and a population level reduction in disease-induced mortality due to changes in the disease dynamics. Both these mechanisms could occur for the population level response to culling for our full model, equations (1-3). In figures 3a(i-ii) & 3b(i-ii) we compare the results from the full model with the demographic effects only model (equations (6)) and in figure 3a(ii) we compare the results from the full model with the disease effects only model (equation (8)), noting that this latter comparison is only valid for DD transmission. The difference between the full model and disease effects only model represents the compensation that is solely due to demographic effects and here this compensation is minimal (figure 3b(i)). The difference between the full model and the demographic effects only model represents the compensation due to the population level reduction in disease-induced mortality and accounts for most of the compensatory growth (figures 3b(i) & 3b(ii)). A key result is that compensation due to disease effects in response to culling can be substantial under both DD and FD transmission.

The effects of culling in populations with virulent infection and recovery to immunity

Figures 1a(iii-iv) & 1b(iii-iv) show that compensatory growth due to a population level release from disease-induced mortality is not evident in systems with life-long immunity following infection. Here, culling leads to a significant reduction in the population density and an increase in infected prevalence (figure 1c(iii-iv)). This effect is most pronounced under FD transmission as here the force of infection remains high when the population abundance is reduced. In systems with life-long immunity the population composition in the absence of culling includes a relatively large proportion of recovered/immune individuals. Culling removes all classes equally, but it takes time for individuals to move through the infection stages to reach the recovered class and therefore culling leads to a larger relative reduction to the recovered class density and so the proportion of the population that suffers virulence (I/N) increases. Figures 4a(i) & 4(ii) show that culling leads to a greater reduction in population density in the full SIR model than in the demographic effects only model. Also, for DD transmission (figure 4b(i)) culling decreases population density less in the full SIR model than in the disease effects only model. Therefore culled populations that support virulent infections with recovery to life-long immunity do not benefit from reduced disease-induced mortality but, as shown here for DD transmission, do exhibit compensation due to demographic effects which mitigate some of the mortality due to culling. A key point is that when there is life-long immunity there can be a significant reduction in the population density and the disease can make the population less resilient to harvesting.

The impact of culling on population management

Culling is often used as a strategy for population eradication, for instance to remove pest or invasive species. We can use our model to investigate how the presence of virulent infection changes the level of culling required to eradicate a population. Figures 3b(i)&(ii) show that in systems without life-long immunity the compensatory effects due to changes in the disease dynamics

mean that an increased level of culling is required to eradicate the population. In systems that have life-long immunity (figures 4b(i) & 4b(ii)) the presence of virulent disease makes the population harder to eradicate under DD transmission but easier to eradicate under FD transmission. Here, under FD transmission, culling leads to an increase in infection prevalence and so increases the population disease-induced mortality in addition to culling mortality. In contrast, under DD transmission, high levels of culling reduce the proportion of recovered individuals to such an extent that the system acts like one in which life-long immunity is absent. Our work therefore indicates that programmes to eradicate invasive species will be hindered if the invasive species harbors a virulent non-immunizing parasite or immunizing parasite under DD transmission but facilitated for strongly immunizing virulent parasites with FD transmission. It is critical therefore to understand the nature of transmission and immunity to the key virulent infectious diseases of a target species prior to the use of culling for population elimination.

The impact of culling on disease management

Culling is also used as a strategy to manage or eradicate a disease. Here the goal may be to eliminate the disease while maintaining viable or maximum levels of host density (Beeton and McCallum 2011; Boadella et al. 2012; Davidson et al. 2009; Hallam and McCracken 2011), or the impact on the host density is of less concern (O'Brien et al. 2011). Our study indicates that the level of culling required to eradicate the disease increases as the virulence increases for DD transmission under both the SI and SIR model frameworks (figures 3c(i) & 4c(i)). Under FD transmission the level of culling required to eradicate the disease increases in the absence of immunity and decreases in the presence of life-long immunity (figures 3c(ii) & 4c(ii)). A key result is that the interval between the level of culling required for disease eradication and population extinction is narrow at high virulence in the absence of immunity and narrow at all levels of virulence with immunity. These results highlight the importance of understanding the infection status of a population before culling for disease management as the level of culling required for disease eradication may put the population at risk of extinction.

Generality of model findings

Our analysis has shown how culling can lead to positive compensatory growth due to a population reduction in disease-induced mortality in systems without immunity and can lead to larger decreases in population density in systems with life-long immunity. It is therefore important to ascertain the threshold in the level of immunity that partitions the positive and negative impacts on growth in response to culling. To do this we examine how the long-term density responds to culling in an SIRS model in which infection leads to immunity but where immunity can wane. For both DD and FD transmission, positive compensatory growth due to infection feedbacks in response to culling occurs except when the recovery rate is high and the loss of immunity is low (figure 5). Therefore, our results indicate that culling can lead to a population level reduction in disease-induced mortality that mitigates the impact of culling on population abundance, provided the infection does not lead to long-lasting immunity.

We confirm our findings for discrete culling in a model of continuous culling (the detailed analysis is presented in online appendix A, section A2 and section A4). The results for the continuous cull model approximate the average density of those for the equivalent discrete cull (online appendix A, figures A1, A3 & A4). As such, the model for continuous culling exhibits the compensation due to a release from disease-induced mortality that we are investigating, although as an average does not show the potential increase in resultant density above the endemic steady state illustrated in figure 3. However, it does allow a robust comparison of steady states for our different model formulations. In particular, we compare the steady states for total density in the full model for DD and FD transmission, N_{DD} and N_{FD} respectively, with the demographic effects only model, N_{dem}, and the disease effects only model, N_{dis}, and compare these values with the density prior to culling, N_e. For the SI model with DD transmission we show that $N_e > N_{DD} > N_{dis} > N_{dem}$ and for FD transmission $N_e > N_{FD} > N_{dem}$, which confirms the findings of figure 3 & online appendix A, figure A2(i). In our illustrated results (online appendix A, figure A2a(i)) we see that $N_{DD} - N_{dem} \gg N_{DD} - N_{dis}$ and therefore the release from disease-

induced mortality contributes most of the compensation in response to culling (a similar result holds for FD transmission, online appendix A, figure A2b(i)). These results also hold for the SIRS model when there is a low rate of recovery or a high rate of loss of immunity. When immunity is sufficiently long-lived (e.g. high recovery and low loss of immunity) then for DD transmission $N_e > N_{dem} > N_{DD} > N_{dis}$ and for FD transmission $N_e > N_{dem} > N_{FD}$, which again confirms the findings in figure 4 & online appendix A, figure A2(ii). These analytical results hold for all valid parameter values and confirm our key finding that the compensation due to disease effects exceeds those due to demographic effects in systems without long-lived immunity.

We also examine the impact of culling that is targeted on infected individuals and find that compensation due to changes in the disease dynamics still occurs under the SI model, but is greater under FD than DD transmission (see online appendix A, section A4 and figure A7). The amplified compensatory growth under FD transmission occurs as targeted culling leads to a direct decrease in the force of infection since infected density decreases more rapidly than total density (under indiscriminate culling infected and total density decrease at the same rate due to culling). For the SIR model targeted culling has little effect on density and prevalence and therefore the negative impacts of culling and disease are no longer observed, but the level of compensation is minimal. For the SIR model targeted culling does initially reduce the force of infection but as a consequence fewer individuals progress to the recovered and immune class; overall these two effects balance. In general, the findings for the model with targeted culling confirm our previous results that compensation due to disease effects occurs in the absence of long-lasting immunity. We also compare the steady states for total density under continuous targeted infected culling for DD and FD transmission, N_{DD}^T and N_{FD}^T respectively. We show that for a sufficient level of targeted infected culling and low rate of recovery or high rate of loss of immunity, then $N_{FD}^T > N_{DD}^T > N_e$, confirming the findings in online appendix A, figures A7 & A8, and supports our finding of the potential for targeted infected culling to induce an over-compensatory population growth response.

The full model (equations (1-3)) includes demographic crowding effects on birth only. In

online appendix A, section A5 we examine the impact of culling on compensatory growth for a version of the full model that can include density-dependent birth and/or death. The results are unchanged under DD transmission regardless of whether density dependence is on birth, death or a combination of both. Under FD transmission the compensatory effect due to a release from disease mortality decreases as the level of density-dependent death increases relative to density-dependent birth. The only scenario in which there is no compensatory effect due to changes in disease dynamics is when there is purely density-dependent death (under FD transmission). Therefore our key finding that culling can lead to compensatory growth due to changes in the disease dynamics is evident for almost all scenarios of density-dependent birth and death. An analytical explanation of these findings is presented in online appendix A, section A5. A parameter sensitivity analysis examining how the level of compensatory growth varies with disease virulence, initial prevalence and cull period is presented in online appendix A, section A6.

Case Study

We highlight the applicability of our findings by considering a case study of the use of culling to manage tuberculosis in Eurasian wild boar (*Sus scrofa*) in central Spain. Here, environmental drivers, such as summer drought, can lead to aggregation with associated high prevalence of infection of *Mycobacterium tuberculosis* complex (MTC) which are the causative agents of animal tuberculosis (TB) (Vicente et al. 2007). We assume that the driver of infection in the wild boar TB system is through environmental contact with free-living MTC pathogen which is shed from the most infectious individuals (Barasona et al. 2017). It is appropriate to assume the population is well-mixed in terms of transmission as on managed estates infection is likely to occur at scarce water holes where free-living MTC can persist and which are utilized frequently by the whole population. Therefore the free-living (FL) transmission mode is used in this case study (see online appendix A, section A3 and recall that FL transmission produces qualitatively similar findings to DD transmission). In central Spain wild boar are the primary reservoir host for MTC and in

some regions up to 70% of the population can be infected with MTC of which half (35% of the total population) may exhibit generalized infection (infected and infectious) (Santos et al. 2015; Vicente et al. 2013). Individuals with generalized infection suffer high levels of disease-induced mortality (Barasona et al. 2017). Since wild boar have an economic and cultural value for the hunting community in Spain there has been a reluctance to use additional culling to control TB as it may result in decreased population abundance. However, since the wild boar TB system is characterized by high disease-induced mortality and no recovery from infection (Barasona et al. 2016) our earlier general results indicate that culling could result in compensatory growth due to reduced disease-induced mortality offsetting the mortality associated with culling and thus sustaining population abundance.

We extend our model framework to represent the wild boar TB systems for a single geographical managed estate containing a homogeneously mixed population covering an area of $3 \times 3\text{km}^2$. The population density of wild boar is separated into different age classes to capture distinct disease and reproductive characteristics for piglets (aged 0-1 year), yearlings (aged 1-2 years), and adults (aged 2 years+). Further, the age-classes are split into susceptible, infected and generalized (infected and infectious) classes to reflect disease status. Yearlings and adults can give birth, and in contrast to our model formulation in equations (1-3) the crowding parameter q (online appendix A, section A7.1), used to limit the disease-free total population density to the carrying capacity, is independent of the endemic disease prevalence. Infection occurs through environmental contact with free-living MTC pathogen which is shed from individuals with the generalized infection. The population dynamics of wild boar and TB are represented by a system of differential equations that are an extension of our general framework, equations (1-3). Full details of the model and parameterization can be found in online appendix A, section A7.

When there is an indiscriminate cull on yearlings and adults the population density shows an initial drop followed by an increase with peak density only falling by 10% in response to a 25% annual cull (figure 6a(i)). While total population size shows only a small reduction there is a more significant reduction in infected individuals and total prevalence drops from 64% to

43% and generalized prevalence from 35% to 22%. More generally (figures 6b(i) & 6c(i)) there is only a shallow decline in population density in response to increased culling up to a threshold at which the disease is eradicated from the system (50% cull). After this the population level declines rapidly. When there is a targeted annual cull of 25% of generalized yearlings and adults (figure 6ii) we see an increase in the total population but only a modest decrease in prevalence and in particular little change in the density of infected and generalized individuals. These results highlight that compensatory growth due to reduced disease-induced mortality may offset increased culling and may lead to a reduction in TB prevalence in wild boar without detrimental reductions in density. Our general predictions may therefore be applicable in this system and highlight the importance of detailed modelling in the context of culling in the face of disease.

Discussion

Despite the ubiquity of infectious disease in nature, there has been little work on the impact of disease on harvested populations. Our key result is that population reductions from culling and harvesting are compensated in a wide range of infectious disease scenarios due to a population level release from disease-induced mortality. The compensatory effect increases as disease virulence, the pre-culling level of prevalence and the level of culling increase and occurs for systems with density-dependent, frequency-dependent and environmental (free-living) modes of transmission. The key outcome is that culling in systems that harbor virulent parasites can lower disease prevalence without significantly reducing, or indeed can increase, population density. The population can therefore be regulated at a similar density by disease or at reduced prevalence by a combination of culling and disease.

Compensation due to changes in disease dynamics occurs in the absence of long-lasting immunity. With long-lasting immunity and indiscriminate culling, disease generally increases the impact of culling and harvesting, reducing the population density compared to systems without the disease. Although there are examples of life-long immunity in wildlife and livestock popula-

tions (rinderpest vaccine produces life-long immunity in African cattle (Roeder et al. 2013)) there are also many examples, including TB, where vaccine-derived immunity wanes (Thom et al. 2012). This indicates that even in those diseases with acquired immunity, this protection may often be partial or wane leading to an SIRS model where individuals become susceptible again after a period of immunity. It is likely therefore that many wildlife systems that support virulent infectious disease will exhibit compensatory growth due to reduced disease-induced mortality following culling. Of course, many populations will have multiple diseases, but the key point is to understand the overall disease burden and in particular whether there is widespread immunity to the key sources of virulence. System-specific models can then determine whether the infectious disease allows increased exploitation or makes the host population more vulnerable. For example, our system-specific model of the wild boar TB interaction in central Spain predicted a strong effect of compensation due to changes in disease dynamics leading to only modest reductions in the population abundance due to hunting. This is therefore an example in which the impact of harvesting is offset in a host that harbors a virulent parasite and suggests hunting is likely to be a sustainable management option in this system.

Our results have important consequences for the use of culling to manage infectious disease. The impact of harvesting on wildlife disease has been previously considered in models with long-lasting immunity (Bolzoni et al. 2007; Choisy and Rohani 2006) which reported an increase in prevalence. Our results confirm these findings since in systems with long-lasting immunity harvesting will reduce the density of immune individuals to a greater proportional extent than other classes (Bolzoni et al. 2007; McCallum 2016). We also support previous studies (Barlow 1996; Potapov et al. 2012; Storm et al. 2013; Wasserberg et al. 2009) which showed that indiscriminate culling is more effective at reducing disease prevalence when infection results from density-dependent rather than frequency-dependent transmission. However, we show that targeted culling is more effective when transmission is frequency-dependent. System-specific models have shown how localized culling could reduce the prevalence of classical swine fever in wild pigs (Cowled et al. 2012) and reduce the prevalence and spread of chronic wasting disease

in white tailed deer (Potapov et al. 2016; Storm et al. 2013), predictions that are supported by observations in the field (Carstensen et al. 2011; Manjerovic et al. 2014).

Our results highlight the difficulty of using culling to eradicate an infectious disease and may explain empirical findings that suggests that culling is not an effective disease management tool. For example, bovine tuberculosis has persisted in badger populations in Great Britain despite comprehensive culling campaigns (Donnelly et al. 2006); Gortázar et al. (2015) reviewed culling programmes worldwide reporting few that achieved 100% efficacy. Theroretical models have suggested that culling could not control white-nose syndrome in bats (Hallam and McCracken 2011); that very high levels of culling were required to eradicate paratuberculosis in rabbits (Davidson et al. 2009) and Tasmanian devil facial tumour disease (Beeton and McCallum 2011); and that culling may increase disease transmission through changes in other ecologically driven factors (Prentice et al. 2014). While our findings indicate that culling can maintain prevalence at reduced levels, they also highlight that high levels of culling are required to eradicate an infection and that there is a narrow range of culling levels between disease eradication and population extinction. System-specific models are therefore required to determine the likelihood of success and the risk of population extinction that may result from culling programmes to control disease.

Previous model studies of the wild boar TB system suggested that culling may contribute to TB management when used in conjunction with other control measures (Anderson et al. 2013). Our model of TB and wild boar shows how such system-specific models can be built to understand when and how culling can be used as a management tool in wildlife systems that harbor virulent disease. Wild boar hunting is a source of income while in some localities spillover of TB into livestock has economic impacts. Our results show that hunting could be a viable method for controlling TB in wild boar because hunting leads to a significant drop in disease prevalence with the model results supported by observations in central Spain (Barasona et al. 2016; Boadella et al. 2012). This is a 'win-win' situation for managed estates since in addition to decrease in disease prevalence a large proportion of the mortality from hunting is countered by a reduction in disease-induced mortality. The model results indicate that the largest decrease in prevalence

and density of infectious individuals is for indiscriminate culling (of juveniles and adults). Here, there is a threshold at which culling eradicated the disease (60% in our model study) after which population abundance decreases rapidly leading to extinction when culling reaches 75%. It may therefore be possible to eradicate TB in wild boar through culling, but it would be critical to determine these thresholds at a regional level. Targeted culling of infectious wild boar resulted in only modest reductions in prevalence and no discernible change in the density of infecteds. This may explain the failure of targeted culling to control TB in empirical studies (Che'Amat et al. 2016).

Over-compensatory population regrowth in response to culling events is well-known in systems that do not consider infectious disease; Abrams and Matsuda (2005) termed this a 'hydra' effect. Abrams (2009) outlined three possible mechanisms that may produce the hydra effect: (i) additional mortality altering pre-existing population oscillations in a way that leads to an increased density, (ii) a temporal separation of mortality and density dependence and (iii) mortality of a consumer leading to over-compensatory changes in other aspects in the food web. Our results for the model with discrete culling show that the resultant density can exceed the original density. Our results with targeted infected culling, for both discrete and continuous model set-ups, show that the resultant density may also surpass the total population density in the absence of culling. These results arise as culling induces population regrowth in an environment with reduced prevalence and therefore reduced disease-induced mortality. Therefore, our novel insight is that the release from mortality caused by endemic disease following culling can also lead to a hydra effect. This has similarities to the hydra effect due to the consumer-resource mechanism (Abrams (2009) mechanism (iii)) where additional mortality of the consumer leads to a reduction in mortality for the resource. Our scenario is different in that it occurs within a single species.

Our key finding is that mortality due to culling in systems that harbor virulent infections may be compensated by reductions in disease-induced mortality. We have also demonstrated that it is important to fully understand the infection processes and to model the specific system before using culling as a disease management tool (Beeton and McCallum 2011). Given the

ubiquity of disease and the importance of harvested populations for food security the novel compensatory mechanism we have identified may help to provide sustainable management of these populations.

Acknowledgments

ET was supported by The Maxwell Institute Graduate School in Analysis and its Applications, a Centre for Doctoral Training funded by the UK Engineering and Physical Sciences Research Council (grant EP/L016508/01), the Scottish Funding Council, Heriot-Watt University and the University of Edinburgh. We wish to thank Y. Michalakis, B. Bolker, A. Hurford and an anonymous referee for helpful comments and guidance in preparing this manuscript.

Appendix A: Supplementary Information and Figures

A1 System steady states and restrictions

We derive expressions for the parameter q and transmission function $\theta(I, N)$ for the full model system (main paper equations (1-3)) by setting the endemic steady state for the total population, $N = N_e$, and the endemic level of infecteds as $I_e = p_i N_e$ where p_i is the initial endemic prevalence of infecteds. This gives the endemic steady states of the system as:

$$I_e = p_i N_e \tag{A1}$$

$$S_e = (1 - \zeta p_i) N_e \tag{A2}$$

$$R_e = (\zeta - 1) p_i N_e \tag{A3}$$

$$\text{where} \quad \zeta = \frac{d + \eta + \gamma}{d + \eta}. \tag{A4}$$

The transmission function $\theta(I, N)$ is then derived as:

$$\text{DD transmission :} \quad \theta(I, N) = \frac{(d + \alpha + \gamma)}{N_e (1 - \zeta p_i)} I \tag{A5}$$

$$\text{FD transmission :} \quad \theta(I, N) = \frac{(d + \alpha + \gamma)}{(1 - \zeta p_i)} \frac{I}{N}. \tag{A6}$$

We also determine an expression for q, the parameter that controls density dependent birth, which is dependent on the constants set for N_e and p_i:

$$q = \frac{b - d - \alpha p_i}{b N_e}. \tag{A7}$$

Given that for valid solutions we must have $q \geq 0$ and $0 \leq p_i \leq 1$, we therefore have a requirement on the system parameters for valid solutions:

$$0 \leq p_i < \frac{(b - d)}{\alpha} \tag{A8}$$

noting that to achieve a non-zero populated steady state in the system we must also have $b > d$. Further to these restrictions, to ensure a positive endemic steady state for the susceptible class

and a positive transmission function, the initial endemic prevalence p_i is also governed by:

$$0 \leq p_i < \frac{d+\eta}{d+\gamma+\eta}. \tag{A9}$$

A2 Continuous culling

In the main paper we have presented results for compensatory growth as a response to discrete culling events. We now consider the same model with continuous culling which approximates the average behaviour of the model with discrete culling. The model with continuous culling allows us to determine conditions for the endemic steady state. We modify main paper equations (1-3) to include continuous culling controlled by the parameters c_S, c_I and c_R for culling susceptibles, infecteds and recovereds respectively:

$$\frac{\mathrm{d}S}{\mathrm{d}t} = Nb(N) - dS - \theta(I,N)S - c_S S + \eta R \tag{A10}$$

$$\frac{\mathrm{d}I}{\mathrm{d}t} = \theta(I,N)S - dI - \alpha I - \gamma I - c_I I \tag{A11}$$

$$\frac{\mathrm{d}R}{\mathrm{d}t} = \gamma I - dR - c_R R - \eta R. \tag{A12}$$

Note we have replaced the explicit term for the birth rate with the more general term $b(N)$. The demographic effects only model (equation (6)) is modified to include the same rate of continuous culling as follows:

$$\frac{\mathrm{d}N}{\mathrm{d}t} = Nb(N) - dN - \alpha p_i N - c_{dem} N \tag{A13}$$

$$\text{where} \quad c_{dem} = c_S\,(1-\zeta p_i) + c_I p_i + c_R(\zeta - 1)p_i. \tag{A14}$$

The disease effects only model (equations (8), (2) & (3)) is modified to include continuous culling by replacing equation (A10) with the following equation in which the birth rate remains constant:

$$\frac{\mathrm{d}S}{\mathrm{d}t} = Nb(N_e) - dS - \theta(I,N)S - c_S S + \eta R. \tag{A15}$$

We restrict the birth function $b(N)$ to be a strictly monotonically decreasing function on the interval $0 \leq N \leq K$ where K is the disease-free steady state for the population ($p_i = 0$) such

that $b(K) = d$. Furthermore we restrict $b(N)$ to be differentiable on $0 \leq N \leq K$ so that

$$\frac{\mathrm{d}b(N)}{\mathrm{d}N} < 0 \tag{A16}$$

on $0 < N < K$. Also, we define the endemic steady state without culling to be N_e such that $0 \leq N_e \leq K$. From equation (A13) we know that

$$b(N_e) = d + \alpha p_i. \tag{A17}$$

We consider steady states for these models under indiscriminate culling ($c_S = c_I = c_R = c$). We want to compare the endemic steady state N_e with the steady states for: the demographic effects only model (equation (A13)), N_{dem}; the disease effects only model (equations (A15), (A11) & (A12)) for DD transmission, N_{dis}; and the full model (equations (A10-A12)) for DD transmission, N_{DD} and FD transmission, N_{FD}. Note that for $c = 0$ all these steady states are all equal to N_e. We wish to compare the steady states in response to culling ($c > 0$).

A2.1 Steady state condition for the demographic effects only model

From equation (A13) we see that for $c > 0$ then

$$b(N_{dem}) = d + \alpha p_i + c > b(N_e) = d + \alpha p_i. \tag{A18}$$

Since $b(N)$ is a strictly monotonically decreasing function then if $b(N_{dem}) > b(N_e)$ it implies that $N_{dem} < N_e$.

A2.2 Steady states for continuous culling with DD transmission

Under DD transmission the steady states for the full DD model and the disease effects only model are:

$$N_{DD} = N_e \left[1 - \zeta p_i\right] \left[1 + \frac{c}{d + \alpha + \gamma}\right] \left[\frac{\alpha}{\alpha + \xi(d + c) - \xi b(N_{DD})}\right] \tag{A19}$$

$$N_{dis} = N_e \left[1 - \zeta p_i\right] \left[1 + \frac{c}{d + \alpha + \gamma}\right] \left[\frac{\alpha}{\alpha + \xi(d + c) - \xi b(N_e)}\right] \tag{A20}$$

$$\text{where} \quad \xi = \frac{d + \eta + c + \gamma}{d + \eta + c}, \qquad \zeta = \frac{d + \eta + \gamma}{d + \eta}. \tag{A21}$$

From A9 we know that $1 - \zeta p_i > 0$. We assume that $\alpha + \xi(d + c) - \xi b(N) > 0$ for $N = N_e$ and $N = N_{DD}$.

A2.2.1 N_{DD} and N_{dis} decrease as γ increases

Rearranging A19 we find that

$$b(N_{DD}) = d + \alpha p_i + c - \frac{\alpha}{\xi}\left[\frac{N_e}{N_{DD}}\frac{(d + \alpha + \gamma + c)}{(d + \alpha + \gamma)}(1 - \zeta p_i) - (1 - \xi p_i)\right]. \tag{A22}$$

We can differentiate A22 with respect to γ and following some algebra it can be shown that

$$\frac{\mathrm{d}N_{DD}}{\mathrm{d}\gamma} < 0 \tag{A23}$$

and therefore N_{DD} decreases as γ increases for all valid parameters.

Using a similar process on equation (A20) where $b(N) = b(N_e)$, which is constant and independent of γ, it follows that

$$\frac{\mathrm{d}N_{dis}}{\mathrm{d}\gamma} < 0 \tag{A24}$$

and so N_{dis} decreases as γ increases for all valid parameters.

A2.2.2 The relationship between N_{DD} and N_e

First we consider the relationship between N_{DD} and N_e. Let us assume that $N_{DD} > N_e$ then from equation (A19)

$$[1 - \zeta p_i]\left[1 + \frac{c}{d + \alpha + \gamma}\right]\left[\frac{\alpha}{\alpha + \xi(d + c) - \xi b(N_{DD})}\right] > 1. \tag{A25}$$

Rearranging equation (A25) we find:

$$b(N_{DD}) > \tag{A26}$$

$$d + \alpha p_i + c\left[\frac{(d + \eta + c)((d + \alpha p_i)(d + \eta) + \gamma(d + \alpha p_i + \eta)) + \gamma(d + \alpha + \gamma)(d + \alpha p_i + \eta)}{(d + \eta)(d + \alpha + \gamma)(d + \gamma + \eta + c)}\right] \tag{A27}$$

and using equation (A17), for the inequality equation (A27) to hold requires that $b(N_{DD}) > b(N_e)$ which contradicts $N_{DD} > N_e$ for $c > 0$. Therefore $N_{DD} < N_e$ for $c > 0$.

A2.2.3 The relationship between N_{DD} and N_{dis}

From section A2.2.2 as $N_{DD} < N_e$ we infer that $b(N_{DD}) > b(N_e)$ for $c > 0$. Therefore for all $c > 0$,

$$\left[\frac{\alpha}{\alpha + \xi(d+c) - \xi b(N_{DD})}\right] > \left[\frac{\alpha}{\alpha + \xi(d+c) - \xi b(N_e)}\right] \tag{A28}$$

and so from equation (A19) and equation (A20) $N_{DD} > N_{dis}$ for all $c > 0$.

A2.2.4 The relationship between N_{DD} and N_{dem}

By definition, N_{DD} equals N_{dem} when

$$b(N_{DD}) = b(N_{dem}) = d + \alpha p_i + c. \tag{A29}$$

Using equation (A22) and equation (A29) we can show that $N_{DD} = N_{dem}$ when,

$$N_{dem} = N_{DD} = N_e \frac{(d+\alpha+\gamma+c)}{(d+\alpha+\gamma)} \frac{(1-\zeta p_i)}{(1-\xi p_i)}. \tag{A30}$$

As $b(N_{dem}) > b(N_e)$ for $c > 0$ it follows that $N_{dem} < N_e$ for $c > 0$, and therefore

$$\frac{(d+\alpha+\gamma+c)}{(d+\alpha+\gamma)} \frac{(1-\zeta p_i)}{(1-\xi p_i)} < 1 \tag{A31}$$

which is only valid for $\gamma > \gamma_{dem0} > 0$ where

$$\gamma_{dem0} = \frac{1}{2p_i}\left[-p_i(d+\eta+c+d+\alpha) + \sqrt{p_i^2(d+\eta+c+d+\alpha)^2 + 4p_i(1-p_i)(d+\eta)(d+\eta+c)}\right] \tag{A32}$$

so that equation (A31) does not hold for $\gamma = 0$, and so $b(N_{DD}|_{\gamma=0})$ cannot equal $d + \alpha p_i + c$ for $c > 0$. From section A2.2.1 we know that $b(N_{DD})$ increases as γ increases, therefore $b(N_{dem}) > b(N_{DD}|_{\gamma=0}) > b(N_e)$ and so $N_{dem} < N_{DD}|_{\gamma=0} < N_e$. It follows that $N_{DD} = N_{dem}$ if $\gamma = \gamma_{dem}$ (where γ_{dem} is the solution to equation (A30)) and $\gamma_{dem} > \gamma_{dem0}$. From section A18 we see that N_{dem} is constant with respect to changes to γ and from section A2.2.1 we know that N_{DD} decreases as γ increases. Therefore $N_{DD} > N_{dem}$ for $\gamma < \gamma_{dem}$ and $N_{DD} < N_{dem}$ for $\gamma > \gamma_{dem}$.

A2.2.5 The relationship between N_{dis} and N_{dem}

We know from A2.2.3 that $N_{dis} < N_{DD}$ for $c > 0$, and therefore from A2.2.4 for sufficiently large γ ($\gamma > \gamma_{dem}$) we know that $N_{dis} < N_{DD} < N_{dem}$. We want to show that for sufficiently small γ that $N_{dis} > N_{dem}$. This can be shown as follows. We know that,

$$N_{dis}\big|_{\gamma=0} = N_e\left[1-p_i\right]\left[1+\frac{c}{d+\alpha}\right]\left[\frac{\alpha}{\alpha(1-p_i)+c}\right]. \tag{A33}$$

Proving the relationship between N_{dem} and N_{dis} when γ is small is algebraically complex. However, substituting $N_{DD} = N_{dis}\big|_{\gamma=0}$ into equation (A22) we find

$$b(N_{dis}|_{\gamma=0}) = d + \alpha p_i + c + c\frac{f(\gamma)}{g(\gamma)} \tag{A34}$$

where $g(\gamma) > 0$ for all valid parameters, and $f(\gamma)$ is a quadratic function. Moreover, $f(0)/g(0) = -1$ and $f(\gamma)$ is a positive parabola. We refer to the positive root of $f(\gamma)$ as γ_{dis0} and this must be the value of γ in equation (A34) such that $N_{dem} = N_{dis}|_{\gamma=0}$. (Note that $\gamma_{dis0} > 0$ as $N_{DD}|_{\gamma=0} > N_{dis}|_{\gamma=0}$). However, as $\gamma_{dem0} > 0$ and we can confirm that $f(\gamma_{dem0}) > 0$ it implies that $\gamma_{dis0} < \gamma_{dem0} < \gamma_{dem}$ and therefore γ_{dis0} does not satisfy equation (A31). Now, as N_{DD} is a decreasing function in γ, it must be that for $\gamma < \gamma_{dis0}$ then $b(N_{dis}|_{\gamma=0}) < b(N_{dem})$ and so $N_{dis}|_{\gamma=0} > N_{dem}$. It follows that as $N_{DD} > N_{dis}$ and as N_{dis} decreases as γ increases, then there exists a threshold $\gamma_{dis} < \gamma_{dem}$ such that when $\gamma < \gamma_{dis}$ then $N_{dis} > N_{dem}$. Therefore for sufficiently low levels of recovery $N_{dis} > N_{dem}$.

A2.3 Steady states for continuous culling with FD transmission

Under FD transmission the steady state, N_{FD}, for the full model satisfies

$$b(N_{FD}) = d + \alpha p_i + c\left[\frac{(d+\eta)(d+\eta+c)(d+\alpha p_i) + \gamma(d+\alpha p_i+\eta)\left[(d+\eta+c)+(d+\alpha+\gamma)\right]}{(d+\eta)(d+\gamma+\eta+c)(d+\alpha+\gamma)}\right]. \tag{A35}$$

A2.3.1 The relationship between N_{FD} and N_e

From equation (A35) and using equation (A17), when $\gamma = 0$ then

$$b(N_{FD}) = d + \alpha p_i + \frac{c(d + \alpha p_i)}{d + \alpha} > b(N_e). \tag{A36}$$

Hence for $\gamma = 0$ we find that $N_e > N_{FD}$. Further, equation (A35) shows that $b(N_{FD})$ increases as γ increases and so $N_e > N_{FD}$ for all $\gamma \geq 0$.

A2.3.2 The relationship between N_{FD} and N_{dem}

We know that $N_{FD} > N_{dem}$ if $b(N_{FD}) < b(N_{dem})$ and using equation (A18) and equation (A35) this requires that

$$\frac{(d+\eta)(d+\eta+c)(d+\alpha p_i) + \gamma(d+\alpha p_i+\eta)\left[(d+\eta+c)+(d+\alpha+\gamma)\right]}{(d+\eta)(d+\gamma+\eta+c)(d+\alpha+\gamma)} < 1 \tag{A37}$$

when $\gamma = 0$ this requires that $(d + \alpha p_i)/(d + \alpha) < 1$ which is true.

For sufficiently large γ and sufficiently small η satisfying the same condition as $N_{DD} < N_{dem}$ in equation (A32) the inequality in equation (A37) can fail and therefore $N_{dem} > N_{FD}$.

A2.4 Conclusion: the relationships between N_e, N_{DD}, N_{FD}, N_{dem} and N_{dis}

Gathering the results from this section, we can say that for diseases with no or short-lived immunity (little or no recovery or high loss of immunity)

$$N_e > N_{DD} > N_{dis} > N_{dem} \tag{A38}$$

$$N_e > N_{FD} > N_{dem} \tag{A39}$$

and for diseases with long-lived immunity (sufficiently high rate of recovery and low loss of immunity),

$$N_e > N_{dem} > N_{DD} > N_{dis} \tag{A40}$$

$$N_e > N_{dem} > N_{FD}. \tag{A41}$$

A2.5 Indiscriminate continuous culling results for $b(N) = b(1 - qN)$

We present results for the continuous model using the same birth function ($b(N) = b(1 - qN)$) as used for the discrete culling results presented in the main paper. We derive the continuous culling rate, c, by equating the steady state for the continuous demographic effects only model, equation (A13) with indiscriminate culling, to the average population density between culling events of the demographic effects only model, equation (6), which has reached a steady state under an annual cull of δ% each year:

$$\frac{b - d - \alpha p_i - c}{bq} = \frac{1}{bq} \ln \left[(1 - \delta) \frac{\exp^{b-d-\alpha p_i} - 1}{1 - \exp^{-(b-d-\alpha p_i)}} \right] \tag{A42}$$

$$\Rightarrow c = \ln \left[\frac{1}{1 - \delta} \right]. \tag{A43}$$

Figures A1a(i) and A1b(i) show the analogous results to those with discrete culling in the main paper (figures 1a(ii) and 1b(ii)). Also, figure A2 shows the analogous results to those with discrete culling (see main paper figure 3 and figure 4). Additionally, for SI models, in figures A3(i) and A3(ii), for DD and FD transmission respectively, we plot the average total population density over the regrowth period following each culling event, illustrating our point that the population density represented by the continuous cull is in close agreement with the average density of the discrete cull. This is again illustrated in figure A4, for different levels of culling, showing the resultant total population density after discrete culling (figure A4a), the average total population density (figure A4b), and the continuous culling steady state (figure A4c) showing again that the resultant average population density is in close agreement with the continuous culling steady state. In all the continuous culling results the population is harvested at continuous rate $c = \log(1/(1 - 0.25))$ to achieve a similar rate of a discrete cull of 25% of the population. For the SI model and DD transmission there is minimal compensation due to demographic effects with the majority of compensatory growth due to the change in disease dynamics (figures A2a(i) & A2b(i)). For FD transmission, the compensation due to the change in disease dynamics is less than for DD transmission (figures A2c(i) & A2d(i)). For the SIR model there is

qualitatively the same level of negative disease compensation as that shown for discrete culling, and a similar level of positive compensatory growth due to demographic effects. Note that results have been plotted here up until the point that the disease endemic steady state becomes invalid ($c = \alpha p_i$), ie. where culling has eradicated the disease. The results for the specific birth function comply with the general results outlined in section A2 and indicate that for indiscriminate culling the findings for discrete and continuous culling are qualitatively similar.

A3 Free living transmission

When we consider free-living infection dynamics we assume that the free-living parasite F is excreted at a constant rate λ by infected individuals and has a decay rate μ. Susceptibles become infected through contact with the free-living parasite such that each susceptible is equally exposed and infection occurs with transmission rate function $\theta_F(F)$. We incorporate this new class into our SI framework (main paper equations (1-3) with $\gamma = 0$), and normalize to achieve the endemic steady state N_e for a particular disease prevalence p_i, such that q takes the same value as the SI model. For this FL model we obtain the following system of ordinary differential equations:

$$\frac{\mathrm{d}S}{\mathrm{d}t} = bN(1 - qN) - dS - \theta_F(F)S \tag{A44}$$

$$\frac{\mathrm{d}I}{\mathrm{d}t} = \theta_F(F)S - dI - \alpha I \tag{A45}$$

$$\frac{\mathrm{d}F}{\mathrm{d}t} = \lambda I - \mu F \tag{A46}$$

$$\theta_F(F) = \frac{\mu}{\lambda}\frac{(d+\alpha)}{N_e\,(1-p_i)}F. \tag{A47}$$

Figure A5 shows that culling populations suffering disease transmitted by free-living particles (equations (A44-A46)) generates a similar compensatory response as seen for DD transmission (figure 1ii). In particular, figure A5c and main paper figure 3b(i) for FL and DD transmission respectively demonstrate that this response is qualitatively similar for all levels of culling.

A4 The impact of targeted culling of infecteds

The results in the main paper focus on indiscriminate culling based on the assumption that identifying infected individuals for a targeted cull is not practicable in most settings. Here we investigate the effect on compensatory growth when only infecteds are targeted for culling. In particular in the continuous model (equations (A10-A12)) we set $c_I > 0, c_S = c_R = 0$.

A4.1 Continuous targeted infected culling steady states

In a similar fashion to section A2 we derive steady state solutions for continuous targeted infecteds culling (equations (A10-A12)) with $c_I > 0, c_S = c_R = 0$) to derive conditions when targeted culling induces over-compensation in the total population.

A4.1.1 Steady states for continuous targeted infected culling with DD transmission

Under DD transmission the steady state, N_{DD}^T, for the full DD model is:

$$N_{DD}^T = N_e \left[1 - \zeta p_i\right] \left[1 + \frac{c_I}{d + \alpha + \gamma}\right] \left[\frac{\alpha + c_I}{\alpha + c_I + \zeta d - \zeta b\left(N_{DD}^T\right)}\right] \tag{A48}$$

$$\text{where} \quad \zeta = \frac{d + \eta + \gamma}{d + \eta}. \tag{A49}$$

Rearranging, we find that for the condition $N_{DD}^T > N_e$ to hold then the following condition on the birth function must also hold:

$$b\left(N_{DD}^T\right) < d + \alpha p_i + \frac{c_I}{\zeta(d + \alpha + \gamma)} \left[\zeta p_i (d + \alpha + \gamma) - (\alpha + c_I)(1 - \zeta p_i)\right]. \tag{A50}$$

By definition if $N_{DD}^T > N_e$ then $b\left(N_{DD}^T\right) < b(N_e)$, therefore for targeted infected culling to induce a rise in population density the culling rate must satisfy the following threshold:

$$c_I > \frac{\zeta p_i (d + \alpha + \gamma) - \alpha(1 - \zeta p_i)}{1 - \zeta p_i}. \tag{A51}$$

Note that this threshold may be < 0 implying that any level of targeted culling will result in an increase in population above the endemic steady state. Also, as γ grows, this culling threshold

grows, ameliorated by the rate of loss of immunity η so that for a sufficiently low rate of recovery or high loss of immunity, targeted culling will result in an increase in population density.

A4.1.2 Steady states for continuous targeted infected culling with FD transmission

Under FD transmission the steady state, N_{FD}^T, for the full model satisfies:

$$b\left(N_{FD}^T\right) = d + \alpha p_i + \frac{c_I}{\zeta(d+\alpha+\gamma)}\left[\zeta p_i(d+\alpha+\gamma) - (1-\zeta p_i)(\alpha+c_I)\right]. \tag{A52}$$

For the condition $N_{FD}^T > N_e$ to hold, we must have $b\left(N_{FD}^T\right) < b(N_e)$, and therefore the level of targeted culling must satisfy:

$$c_I > \frac{\zeta p_i(d+\alpha+\gamma) - \alpha(1-\zeta p_i)}{1-\zeta p_i} \tag{A53}$$

the same condition as for DD transmission (equation (A51)). Therefore targeted infected culling under FD transmission will induce a rise in population density under the same model conditions as DD transmission.

A4.1.3 The relationship between N_{DD}^T and N_{FD}^T

We can further examine the relationship between N_{DD}^T and N_{FD}^T. Rearranging equation (A48) and from equation (A52) we find that:

$$b\left(N_{DD}^T\right) - b\left(N_{FD}^T\right) = \left[1 - \frac{N_e}{N_{DD}^T}\right]\frac{(\alpha+c_I)(1-\zeta p_i)(d+\alpha+\gamma+c_I)}{\zeta(d+\alpha+\gamma)}. \tag{A54}$$

From equation (A54) we see that when $N_{DD}^T > N_e$ (for the appropriate level of c_I specified by equations (A51) and (A53)) then $b\left(N_{DD}^T\right) - b\left(N_{FD}^T\right) > 0$ and therefore for sufficiently large targeted infected culling (which is more likely when there is low recovery to immunity or high loss of immunity), $N_{FD}^T > N_{DD}^T$. When $N_{DD}^T < N_e$ (when c_I does not satisfy the threshold specified by equations (A51) and (A53)) then $b\left(N_{DD}^T\right) - b\left(N_{FD}^T\right) < 0$ and therefore when targeted culling is sufficiently low, or there is sufficiently high recovery to immunity and sufficiently low loss of immunity, $N_{FD}^T < N_{DD}^T$.

A4.1.4 Conclusion, the relationships between N_{DD}^T, N_{FD}^T and N_e

In summary, for diseases with no or short-lived immunity and a sufficient level of targeted infected culling

$$N_{FD}^T > N_{DD}^T > N_e \tag{A55}$$

and so continuous culling can lead to an increase in population density.

A4.2 Targeted infected continuous culling results for $b(N) = b(1 - qN)$

For illustration, we present results for the discrete and continuous model using the same birth function ($b(N) = b(1 - qN)$) as used for the discrete culling results presented in the main paper. Figures A6 and A7 show the population response for discrete targeted culling for both SI and SIR models with DD and FD transmission. Note the same culling rate is used in indiscriminate culling and targeted culling, so that the culling effort is the same however there are a greater number of individuals culled during indiscriminate culling. Also, for discrete targeted culling, we also modify the rate of culling in the demographic effects only model to be multiplied by p_i to remove the equivalent number of infecteds at the endemic steady state. For the SI model targeting infecteds only for DD transmission leads to compensatory growth (figure A6a(i) & figure A7a(i)), but the compensatory effect is lower than with indiscriminate culling. For FD transmission (figure A6b(i) & figure A7b(i)), culling infecteds causes a greater release from disease-induced mortality as this causes a greater reduction in the force of infection. This leads to increased compensatory growth and a greater reduction in disease prevalence than for indiscriminate culling (figure A6c(i) black line).

For the SIR model, targeting infecteds brings no resultant compensatory growth for discrete culling (figures A7a(ii) & A7b(ii)), but also does not cause large population depletion (figure A6a(ii) & A6b(ii)) as with indiscriminate culling. This is the same for both DD transmission and FD transmission. This is because targeted culling does not deplete the level of recovered and immune individuals in the population.

In the continuous model with targeted culling ($c_I > 0, c_S = c_R = 0$) the steady states can be determined analytically. For DD transmission these are

$$S^T_{DD} = \frac{d+\alpha+\gamma+c_I}{\beta} \qquad \text{where} \quad \beta = \frac{d+\alpha+\gamma}{N_e\left(1-p_i\frac{d+\gamma}{d}\right)} \tag{A56}$$

$$N^T_{DD} = \frac{d}{2bq(\gamma+d)}\left[b\frac{d+\gamma}{d} - d - \alpha - \gamma - c_I + \right. \tag{A57}$$

$$\left. \sqrt{\left(b\frac{d+\gamma}{d} - d - \alpha - \gamma - c_I\right)^2 + 4bqS^T_{DD}\frac{\gamma+d}{d}(\alpha+c_I)}\right]. \tag{A58}$$

The total population steady state for the demographic effects only model is:

$$N^T_{dem} = \frac{b-d-\alpha p_i - p_i c_I}{bq}. \tag{A59}$$

The steady state for the disease effects only model is:

$$S^T_{dis} = \frac{d+\alpha+\gamma+c_I}{\beta} \qquad \text{where} \quad \beta = \frac{d+\alpha+\gamma}{N_e\left(1-p_i\frac{d+\gamma}{d}\right)} \tag{A60}$$

$$N^T_{dis} = S^T_{dis}\frac{d(\alpha+c_I)}{d(d+\alpha+\gamma+c_I) - (\gamma+d)b(1-qN_e)}. \tag{A61}$$

For FD transmission and targeted culling the steady state is:

$$S^T_{FD} = \frac{(d+\alpha+\gamma+c_I)^2}{bq\beta^2}\left[\frac{b\beta}{d+\alpha+\gamma+c_I} + \frac{d}{d+\gamma}(\alpha+c_I-\beta)\right] \tag{A62}$$

$$N^T_{FD} = \frac{\beta}{(d+\alpha+\gamma+c_I)}S^T_{FD} \qquad \text{where} \quad \beta = \frac{d+\alpha+\gamma}{\left(1-p_i\frac{d+\gamma}{d}\right)}. \tag{A63}$$

Figure A8 shows the same set of results for the total population steady states as figure A2 with targeted culling of infecteds. For the SI model as the culling rate of infecteds increases, compensation due to the change in disease dynamics also increases under DD transmission (figures A8a(i) & A8b(i)) and to a greater extent under FD transmission (figures A8c(i) & A8d(i)). For DD transmission we again note that disease effects drive the majority of the compensation in response to culling. For the SIR model for DD transmission (figures A8a(ii) & A8b(ii)) both the full model and the demographic effects only model show no change in steady state density as the targeted

culling of infecteds grows, however the disease effects only steady population density reduces as targeted culling of infecteds grows. For FD transmission (figures A8c(ii) & A8d(ii)) there is no compensatory growth due to disease dynamics. We note that in our illustrative results we set parameters $\alpha = 4$, $d = 0.5$, $p_i = 0.1$, $c_I = 0.25$, $\eta = 0$ and $\gamma = 0$ or $\gamma = 4$ for SI or SIR models respectively. The threshold specified in equation (A51) is therefore $c_I > 0$ for SI models and $c_I > 72.5$ for SIR models and therefore predict that there will be over-compensation for the SI results and not for the SIR results as shown in the figures. The results for continuous targeted culling confirm the results for targeted culling in the discrete model (figure A7).

A5 Density dependent mortality

Our system formulation (main paper equations (1-3)) models the population growth function with density dependent birth. To examine whether density dependent death impacts the compensatory growth effect that we present in the main paper we also consider results for a similarly formulated system that includes density dependent death. We modify equations (1-3) to include non-negative parameters q_b and q_d which control the levels of density dependent birth and death (notably a positive q_d indicating a level of density dependent death):

$$\frac{\mathrm{d}S}{\mathrm{d}t} = b(1 - q_b N)N - d(1 + q_d N)S - \theta_D(I, N)S \tag{A64}$$

$$\frac{\mathrm{d}I}{\mathrm{d}t} = \theta_D(I, N)S - d(1 + q_d N)I - \alpha I - \gamma I \tag{A65}$$

$$\frac{\mathrm{d}R}{\mathrm{d}t} = \gamma I - d(1 + q_d N)R. \tag{A66}$$

Considering the system without recovery (an SI framework), but maintaining the same disease-free steady state and endemic steady state $N = N_e$ where $I_e = p_i N_e$ and $S_e = (1 - p_i)N_e$, the transmission function $\theta_D(I, N)$ is defined for DD and FD transmission as:

$$\text{DD transmission}: \quad \theta_D(I, N) = \frac{(d\,(1 + q_d N_e) + \alpha)}{N_e\,(1 - p_i)} I = \frac{(b\,(1 - q_b N_e) + (1 - p_i)\alpha)}{N_e\,(1 - p_i)} I \tag{A67}$$

$$\text{FD transmission}: \quad \theta_D(I, N) = \frac{(d\,(1 + q_d N_e) + \alpha)}{(1 - p_i)} \frac{I}{N} = \frac{(b\,(1 - q_b N_e) + (1 - p_i)\alpha)}{(1 - p_i)} \frac{I}{N}. \tag{A68}$$

where, to achieve the required steady states, q_b and q_d must satisfy:

$$q_d = \frac{b - d - \alpha p_i - b q_b N_e}{d N_e} \tag{A69}$$

$$0 \leq q_b \leq \frac{b - d - \alpha p_i}{b N_e}. \tag{A70}$$

q_b and q_d are therefore constrained by each others value in this model such that when q_b takes values between 0 to $(b - d - \alpha p_i)/(bN_e)$, correspondingly q_d takes values from $(b - d - \alpha p_i)/(dN_e)$ to 0. Thus, when $q_b = 0$ we have a system with only density dependent death, when $0 < q_b < (b - d - \alpha p_i)/(bN_e)$ we have a system with both density dependent birth and density dependent death and when $q_b = (b - d - \alpha p_i)/(bN_e)$ then $q_d = 0$ and we recover our original model formulation with only density dependent birth.

Varying values of q_b from 0 to $(b - d - \alpha p_i)/(bN_e)$ (i.e. from having zero density dependence on birth and density dependent death only to zero density dependence on death and density dependent birth only) we examine the effect of the difference between the model that includes epidemiological dynamics (equations (A64-A66)) and a corresponding demographic effects only model containing the equivalent density dependent birth and death formulations as follows:

$$\frac{\mathrm{d}N}{\mathrm{d}t} = bN(1 - q_b N) - d(1 + q_d N)N - \alpha p_i N. \tag{A71}$$

Figure A9 shows that culling generates compensatory growth due to disease dynamics regardless of the level of density dependent birth relative to density dependent death except in the singular case where there is density dependent death only under FD transmission. Figure A9a shows that varying q_b has no effect on the resultant population density following culling for DD transmission. The results reported in the main text therefore hold under DD transmission. Our results also hold under FD transmission except in the singular case when $q_b = 0$, indicating that there is density dependent death only.

A5.1 Why the demographic effects only model remains invariant to changes in q_b

Figure A9a shows that for the demographic effects only model (equation (A71)), the resultant population density following the culling regime does not vary as q_b varies. To explain this we substitute equation (A69) into the demographic effects only model (equation (A71)) as follows:

$$\frac{\mathrm{d}N}{\mathrm{d}t} = bN(1-q_bN) - d(1+q_dN)N - \alpha p_i N \tag{A72}$$

$$= bN - N^2\left(bq_b + \frac{b-d-\alpha p_i - bq_bN_e}{N_e}\right) - dN - \alpha p_i N \tag{A73}$$

$$= bN - \frac{b-d-\alpha p_i}{N_e}N^2 - dN - \alpha p_i N \tag{A74}$$

$$= bN\left(1 - \frac{b-d-\alpha p_i}{bN_e}N\right) - dN - \alpha p_i N. \tag{A75}$$

and thus we recover the original demographic effects only model from the main paper (equation (6)). This shows that the change in population for this new formulation of the demographic effects model (equation (A71)) does not vary as q_b varies and therefore does not exhibit any change in behaviour from the original demographic effects only model (equation (6)) in response to culling.

A5.2 Density dependent mortality with FD transmission

To understand why the model with FD transmission and no density dependent birth ($q_b = 0$) does not show any additional compensatory growth above the demographic effects only model (equation (A71)) we examine the rate of change of the disease prevalence for equations (A64-A66).

$$\frac{\mathrm{d}}{\mathrm{d}t}\left(\frac{I}{N}\right) = \frac{N\frac{\mathrm{d}I}{\mathrm{d}t} - I\frac{\mathrm{d}N}{\mathrm{d}t}}{N^2} \tag{A76}$$

$$= \frac{1}{N^2}\left[N\left(\theta_D S - d(1+q_dN)I - \alpha I\right) - I\left(b(1-q_bN)N - d(1+q_dN) - \alpha I\right)\right] \tag{A77}$$

$$= \frac{1}{N^2}\left[\theta_D SN - \alpha I(N-I) - bNI(1-q_bN)\right] \tag{A78}$$

$$= \frac{I}{(1-p_i)N^2}\left[-b(I-p_iN) - bq_b(N_eS - N^2(1-p_i))\right]. \tag{A79}$$

We see that when $q_b = 0$, an initial condition that satisfies $I = p_i N$ will give a solution that does not vary from this initial prevalence. Therefore, as our culling regime starts with an initial prevalence p_i, the prevalence of the disease throughout the culling regime does not change and therefore culling does not yield any compensatory growth due to reduction in disease mortality. Therefore the full model matches the demographic effects only model. When $q_b > 0$, we note that after an initial cull when the disease prevalence is still p_i (so that $I = p_i N$), the first term in equation (A79) is zero and the second term is negative indicating that after the initial cull the prevalence will start to decrease leading to a reduction in disease-induced mortality in the population, supporting our results in the main paper.

A5.3 Density dependent mortality with DD transmission

Our result in figure A9 for DD transmission shows varying q_b does not affect the compensatory growth response to culling. We explain this by examining the rate of change of the population density N:

$$\frac{\mathrm{d}N}{\mathrm{d}t} = b(1 - q_b N)N - d(1 + q_d N)N - \alpha I \tag{A80}$$

$$= bN - bq_b N^2 - N\left[b - (b - d) + \frac{N}{N_e}(b - d - \alpha p_i - bq_b N_e)\right] - \alpha I \tag{A81}$$

$$= N\left[(b - d) - \frac{N}{N_e(b - d - \alpha p_i)}\right] - \alpha I \tag{A82}$$

which shows that the growth in population density is independent of the density dependent birth and death parameters, q_b and q_d. Therefore varying q_b has no effect on the population rate of regrowth following a cull. To compare with FD transmission we also examine the rate of

change of the disease prevalence:

$$\frac{\mathrm{d}}{\mathrm{d}t}\left(\frac{I}{N}\right) = \frac{N\frac{\mathrm{d}I}{\mathrm{d}t} - I\frac{\mathrm{d}N}{\mathrm{d}t}}{N^2} \tag{A83}$$

$$= \frac{1}{N^2}\left[N\left(\theta_D S - d(1+q_d N)I - \alpha I\right) - I\left(b(1-q_b N)N - d(1+q_d N) - \alpha I\right)\right] \tag{A84}$$

$$= \frac{1}{N^2}\left[\theta_D SN - \alpha I(N-I) - bNI(1-q_b N)\right] \tag{A85}$$

$$= \frac{I}{N^2}\left[\frac{(b - bq_b N_e + \alpha(1-p_i))}{(1-p_i)N_e}SN - \alpha(N-I) - bN + bq_b N^2\right] \tag{A86}$$

$$= \frac{I}{N^2(1-p_i)N_e}\Big[-bN((1-p_i)N_e - S) - \tag{A87}$$

$$bq_b N_e N(S - (1-p_i)N) - \alpha(1-p_i)S(N_e - N)\Big] \tag{A88}$$

noting in equation (A88), given the maximum value of q_b, that the first term is negative whilst S remains below the endemic susceptible density, the second term is negative whilst the infected prevalence is lower than the endemic prevalence and the third term is negative when N is below the total population endemic steady state. From this we can determine that a cull taking the population below the endemic steady state, and the susceptibles below the endemic susceptible density must lead to a reduction in disease prevalence, which therefore leads to a reduction in the proportion of the population suffering disease-induced mortality, supporting our results in the main paper.

A6 Parameter sensitivity

In figure A10 we undertake a parameter sensitivity analysis to assess the magnitude of the compensatory effect for a range of model parameters in the SI and SIR model framework: the level of disease-induced mortality α; the initial endemic prevalence p_i; and the cull period (the length of time between each sequential cull event). As intuitively expected for the SI model framework the compensatory effect (the difference between the dotted lines and solid line in figure A10) increases as virulence increases (figure A10a(i)) and as the initial disease prevalence, p_i, increases (figure A10b(i)) and as the culling period decreases (the frequency of culling increases) (figure A10c(i)). For the SIR model with FD transmission the disease induced negative impact of

culling increases as the virulence and initial infected prevalence increases whereas there is less change in the impact under DD transmission (figures A10a(ii) & A10b(ii)). The compensatory effect shows only low sensitivity to changes in the cull period for DD and FD transmission in the SIR model (figure A10c(ii)).

A7 Wild boar TB model

We introduce a mathematical model that can represent the key processes influencing TB infection in wild boar in Spain. Our model reflects a single geographical managed estate containing a homogeneously mixed population covering an area representative of a hunting estate. The population density of wild boar is separated into different age classes to capture distinct disease and reproductive characteristics for piglets (aged 0-1 year) P, yearlings (aged 1-2 years) Y, and adults (aged 2 years+) A. Further, the age-classes are split into susceptible, infected and generalized (super-shedder) classes (subscripts S, I, G, respectively) to reflect the disease status of the population. The population dynamics of the wild boar TB system are represented by the following set of non-linear differential equations (which is an extension of classical disease modelling frameworks (Anderson and May 1981; Keeling and Rohani 2008):

$$\frac{dP_S}{dt} = (b_Y(Y_S + Y_I) + b_A(A_S + A_I) + b_G(Y_G + A_G))(1 - qN) - mP_S - d_P P_S - \beta_P P_S F \quad \text{(A89)}$$

$$\frac{dP_I}{dt} = \beta_P P_S F - mP_I - d_P P_I - \varepsilon_P P_I \quad \text{(A90)}$$

$$\frac{dP_G}{dt} = \varepsilon_P P_I - mP_G - d_P P_G - \alpha P_G \quad \text{(A91)}$$

$$\frac{dY_S}{dt} = mP_S - mY_S - d_Y Y_S - \beta_Y Y_S F \quad \text{(A92)}$$

$$\frac{dY_I}{dt} = \beta_Y Y_S F + mP_I - mY_I - d_Y Y_I - \varepsilon_Y Y_I \quad \text{(A93)}$$

$$\frac{dY_G}{dt} = \varepsilon_Y Y_I + mP_G - mY_G - d_Y Y_G - \alpha Y_G \quad \text{(A94)}$$

$$\frac{dA_S}{dt} = mY_S - d_A A_S - \beta_A A_S F \quad \text{(A95)}$$

$$\frac{dA_I}{dt} = \beta_A A_S F + mY_I - d_A A_I - \varepsilon_A A_I \quad \text{(A96)}$$

$$\frac{dA_G}{dt} = \varepsilon_A A_I + mY_G - d_A A_G - \alpha A_G \quad \text{(A97)}$$

$$\frac{dF}{dt} = \lambda(P_G + Y_G + A_G) - \mu F. \quad \text{(A98)}$$

Here, N represents the total wild boar population. Susceptible and infected yearlings and adults give birth to susceptible piglets at rates b_Y and b_A respectively. Generalized yearlings and adults give birth to piglets at rate b_G. The total population is regulated through a crowding parameter, q, that acts to stabilize the total population to a carrying capacity, $N = K$, in the absence of disease. Maturity from piglets to yearlings and yearlings to adults occurs at rate m and piglets, yearlings and adults may die of natural causes at rates d_P , d_Y , d_A respectively. Here we assume $d_P = d_Y = d_A$.

The prime driver for infection in the wild boar TB system is through environmental contact with free-living MTC particles, with density F. We assume that free-living particles are shed from generalized wild boar at rate λ and decay at rate μ. Susceptibles may become infected

through contact with free-living MTC particles with transmission coefficients β_P, β_Y and β_A and infecteds can progress to the generalized class at rates ε_P, ε_Y and ε_A for the different age classes respectively. We assume that individuals in the generalized class suffer an additional disease-induced mortality at rate α. We assume piglets and yearlings are more susceptible to MTC infection than adults and so set $\beta_P = \beta_Y$, which we assume to be three times greater than transmission for adults, $\beta_A = 3\beta_Y$. Similarly we set the rate of progression to generalized infection for piglets and yearlings to be the same, $\varepsilon_P = \varepsilon_Y$, and three times the rate for adults, $\varepsilon_Y = 3\varepsilon_A$. In this way we have set the model so that the yearling class is the same as the piglet class in terms of disease characteristics, but the yearling class is the same as the adult class in terms of reproductive processes.

A7.1 Wild boar TB model parameters

We set the model parameters to be representative of the wild boar TB system in Central Spain (Díez-Delgado et al. 2018). The parameters are as follows:

$b_Y = b_A = b_G = \log(4)$ The population birth rate in a disease-free population when resources are unlimited. This constant rate means that for each reproductive member of the population, 3 piglets will be born, averaged over the population over a year. (This has been derived by assuming that there is a 50% sex ratio and that each female produces an average of 6 offspring per year when resources are not limited.) Units: $year^{-1}$.

$K = 500$ The carrying capacity for the total population in the target area in the absence of disease. Units: $population \times area^{-1}$.

$q = (1 - d_A(d_P + m)(d_Y + m)/(m\,(b_A m + b_Y d_A)))\,/K$ This parameter limits the total population to the carrying capacity K in the populated disease-free steady state, and is derived from steady-state analysis of the model without infection. Units: $density^{-1}$.

$m = 1$ The rate that piglets mature to yearlings and yearlings mature to adults. These rates assume that it takes on average 1 year to enter the next age class. Units: $year^{-1}$.

$d_P = d_Y = d_A = 1/7$ The natural death rate of all classes which implies an average life expectancy of 7 years. Units: $year^{-1}$.

$\beta_P = \beta_Y = c_\beta \beta_A = 20/K$ The infection rates are fitted to give prevalence levels observed in the wild boar TB system in central Spain. We assume that $c_\beta = 3$ and so disease transmission to piglets and yearlings is three times that of the adult rate under the assumption that transmission is higher for piglets and yearlings than it is for adults. Units: $density^{-1} \times year^{-1}$.

$\varepsilon_P = \varepsilon_Y = 2$ The rate that infected piglets and yearlings become generalized. This assumes that it takes on average 6 months for an infected piglet or yearling to progress to the generalized class. Units: $year^{-1}$.

$\varepsilon_A = 2/3$ This is the rate that infectious adults become generalized. This assumes that it takes on average 18 months for an infected adult to progress to the generalized class. Units: $year^{-1}$.

$\alpha = 1$ This is the additional disease induced death rate of the generalized class and assumes that on average individuals spend 1 year in the generalized class before death. Units: $year^{-1}$.

$\lambda = 1$ The rate of shedding of infectious particles by generalized classes. We normalize this value to 1. This is valid as we have explored a range of values for β_P, β_Y and β_A which scale with the size of λ and the density of free-particles, F. Units: $year^{-1}$.

$\mu = 6$ This is the decay rate for free-living particles, indicating that they have an average life expectancy of 2 months. Units: $year^{-1}$.

Literature Cited

Abrams, P. A. 2009. When does greater mortality increase population size? The long history and diverse mechanisms underlying the hydra effect. Ecology Letters 12:462–474.

Abrams, P. A., and H. Matsuda. 2005. The effect of adaptive change in the prey on the dynamics of an exploited predator population. Canadian Journal of Fisheries and Aquatic Sciences 62:758–766.

Anderson, R., and R. May. 1979. Population biology of infectious diseases 1. Nature 280:361–367.

Anderson, R., and R. May. 1981. The population dynamics of microparasites and their invertebrate hosts. Philosophical Transactions of the Royal Society B 291:451–524.

Anderson, L., C. Gortázar, J. Vicente, M. Hutchings, and P. White. 2013. Modelling the effectiveness of vaccination in controlling bovine tuberculosis in wild boar. Wildlife Research 40(5):367–376.

Barasona, J., P. Acevedo, I. Díez-Delgado, J. Queiros, R. Carrasco-García, C. Gortázar, and J. Vicente. 2016. Tuberculosis-associated death among adult wild boars, Spain, 2009–2014. Emerging infectious diseases 22:2178–2180.

Barasona, J., J. Vicente, I. Díez-Delgado, J. Aznar, C. Gortázar, and M. Torres. 2017. Environmental presence of *Mycobacterium tuberculosis* complex in aggregation points at the wildlife/livestock interface. Transboundary and emerging diseases 64(4):1148–58.

Barlow, N. 1996. The ecology of wildlife disease control: simple models revisited. Journal of Applied Ecology 33:303–314.

Beeton, N., and H. McCallum. 2011. Models predict that culling is not a feasible strategy to prevent extinction of Tasmanian devils from facial tumour disease. Journal of Applied Ecology 48:1315–1323.

Boadella, M., J. Vicente, F. Ruiz-Fons, J. de la Fuente, and C. Gortázar. 2012. Effects of culling eurasian wild boar on the prevalence of *Mycobacterium bovis* and Aujeszky's disease virus. Preventive Veterinary Medicine 107:214–221.

Bolzoni, L., L. Real, and G. De Leo. 2007. Transmission heterogeneity and control strategies for infectious disease emergence. PLoS One, 2:e747.

Carstensen, M., D. J. O'Brien, and S. Schmitt. 2011 Public acceptance as a determinant of management strategies for bovine tuberculosis in free-ranging US wildlife. Veterinary Microbiology 151:200–204.

Che'Amat, A., J. A. Armenteros, D. Gonzalez-Barrio, J. F. Lima, I. Díez-Delgado, J. A. Barasona, B. Romero, K. P. Lyashchenko, J. A. Ortiz, and C. Gortázar. 2016. Is targeted removal a suitable means for tuberculosis control in wild boar? Preventive veterinary medicine pages 132–135.

Choisy, M. and P. Rohani. 2006. Harvesting can increase severity of wildlife disease epidemics. Proceedings of the Royal Society of London B: Biological Sciences 273:2025–2034.

Cowled, B., M. Garner, K. Negus, and M. Ward. 2012. Controlling disease outbreaks in wildlife using limited culling: modelling classical swine fever incursions in wild pigs in Australia. Veterinary Research 43:3.

Davidson, R., G. Marion, P. White, and M. Hutchings. 2009. Use of host population reduction to control wildlife infection: rabbits and paratuberculosis. Epidemiology & Infection 137:131–138.

Díez-Delgado, I., I. A. Sevilla, B. Romero, E. Tanner, J. A. Barasona, A. R. White, P. W. Lurz, M. Boots, J. de la Fuente, L. Dominguez, and J. Vicente. 2018. Impact of piglet oral vaccination against tuberculosis in endemic free-ranging wild boar populations. Preventive Veterinary Medicine 155:11–20.

Donnelly, C. A. , R. Woodroffe, D. Cox, F. J. Bourne, C. Cheeseman, R. S. Clifton-Hadley, G. Wei,

G. Gettinby, P. Gilks, H. Jenkins, and W. T. Johnston. 2006. Positive and negative effects of widespread badger culling on tuberculosis in cattle. Nature 439(7078):843.

Gortázar, C.,I. Díez-Delgado, J. A. Barasona, J. Vicente, J. De La Fuente and M. Boadella. 2015. The wild side of disease control at the wildlife-livestock-human interface: a review. Frontiers in Veterinary Science 1:27.

Hallam, T., and G. McCracken. 2011. Management of the panzootic white–nose syndrome through culling of bats. Conservation Biology 25:189–194.

Keeling, M. J., and P. Rohani. 2008. Modeling infectious diseases in humans and animals. Princeton University Press, Princeton, NJ.

Manjerovic, M., M. Green, N. Mateus-Pinilla, and J. Novakofski. 2014. The importance of localized culling in stabilizing chronic wasting disease prevalence in white-tailed deer populations. Preventive Veterinary Medicine 113:139–145.

McCallum, H. 2016. Models for managing wildlife disease. Parasitology 143:805–820.

O'Brien, D. J., S. M. Schmitt, B. A. Rudolph, and G. Nugent. 2011. Recent advances in the management of bovine tuberculosis in free-ranging wildlife. Veterinary Microbiology, 151(1-2):23–33.

Potapov, A., E. Merrill, and M. Lewis. 2012. Wildlife disease elimination and density dependence. Proceedings of the Royal Society of London B: Biological Sciences 279:3139–3145.

Potapov, A., E. Merrill, M. Pybus, and M. Lewis. 2016. Chronic wasting disease: Transmission mechanisms and the possibility of harvest management. PloS One 11:e0151039.

Prentice, J. C., G. Marion, P. C. White, R. S. Davidson, and M. R. Hutchings. 2014. Demographic processes drive increases in wildlife disease following population reduction. PloS One 9(5):e86563.

Ricker, W. 1954. Stock and recruitment. Journal of the Fisheries Board of Canada 11:559–623.

Roeder, P., J. Mariner, and R. Kock. 2013. Rinderpest: the veterinary perspective on eradication. Philosophical Transactions of the Royal Society B 368:20120139.

Santos, N., V. Almeida, C. Gortázar, and M. Correia-Neves. 2015. Patterns of mycobacterium tuberculosis-complex excretion and characterization of super-shedders in naturally-infected wild boar and red deer. Veterinary Research 46:129.

Storm, D., M. Samuel, R. Rolley, P. Shelton, N. Keuler, B. Richards, and T. Van Deelen. 2013. Deer density and disease prevalence influence transmission of chronic wasting disease in white-tailed deer. Ecosphere 4:1–14.

Thom, M., M. McAulay, H. Vordermeier, D. Clifford, R. Hewinson, B. Villarreal-Ramos, and J. Hope. 2012. Duration of immunity against Mycobacterium bovis following neonatal vaccination with bacillus Calmette-Guérin Danish: significant protection against infection at 12, but not 24, months Clinical and Vaccine Immunology 19:1254–1260.

Uehlinger, F., A. Johnston, T. Bollinger, and C. Waldner. 2016. Systematic review of management strategies to control chronic wasting disease in wild deer populations in North America. BMC veterinary research 12:173.

Vicente, J., U. Höfle, J. Garrido, P. Acevedo, R. Juste, M. Barral, and C. Gortázar. 2007. Risk factors associated with the prevalence of tuberculosis-like lesions in fenced wild boar and red deer in south central spain. Veterinary Research 38(3):451–464.

Vicente, J., J. Barasona, P. Acevedo, J. Ruiz-Fons, M. Boadella, I. Díez-Delgado, B. Beltran-Beck, and C. Gortázar. 2013. Temporal trend of tuberculosis in wild ungulates from Mediterranean Spain Transboundary and Emerging Diseases 60(s1):92–103.

Wasserberg, G., E. Osnas, R. Rolley, and M. Samuel. 2009. Host culling as an adaptive man-

agement tool for chronic wasting disease in white-tailed deer: a modelling study. Journal of Applied Ecology 46:457–466.

Woodroffe, R. 1999. Managing disease threats to wild mammals. Animal Conservation forum 2:185–193.

Figure legends

Online figure legends

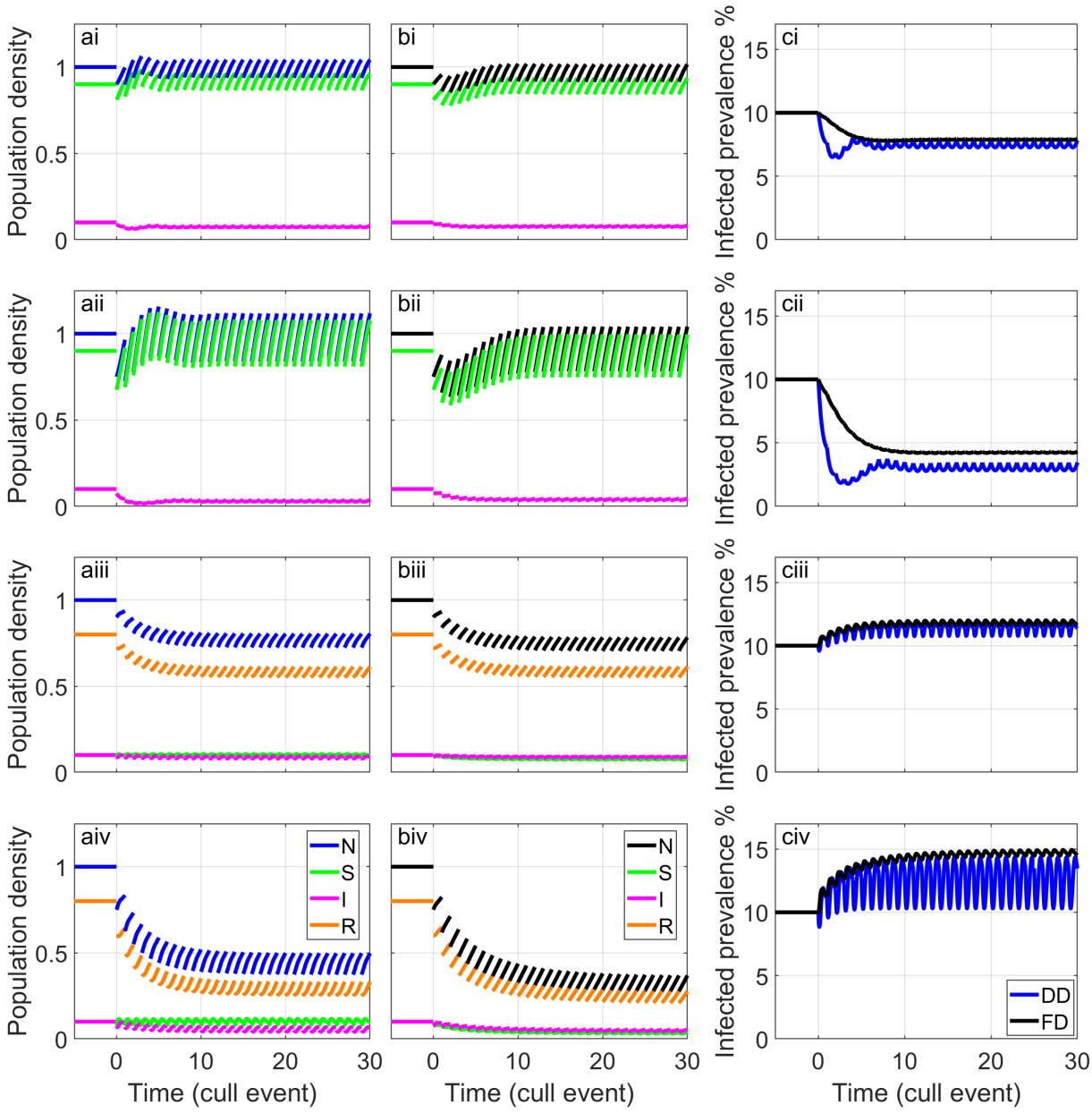

Figure 1: The population density and infected prevalence (I/N) response to culling for equations (1-3). (i),(ii) show results for the SI model, (iii),(iv) show results for the SIR model. Results are shown for a 10% cull (i,iii) and a 25% cull (ii,iv). (a) shows DD transmission and (b) FD transmission. (a) and (b) show the total density of susceptibles (green); the total density of infected (magenta); the total density of recovered/immune (orange); and the total populations density (blue for DD (a), black for FD (b)). (c) shows the disease prevalence for DD (blue) and FD (black) transmission. Results are shown for a virulent infection, $\alpha = 4$, and with an initial endemic disease prevalence of $p_i = 10\%$. Other parameters are: $b = 1.6$, $d = 0.5$; for (i) and (ii) $\gamma = 0$; and (iii),(iv) $\gamma = 4$.

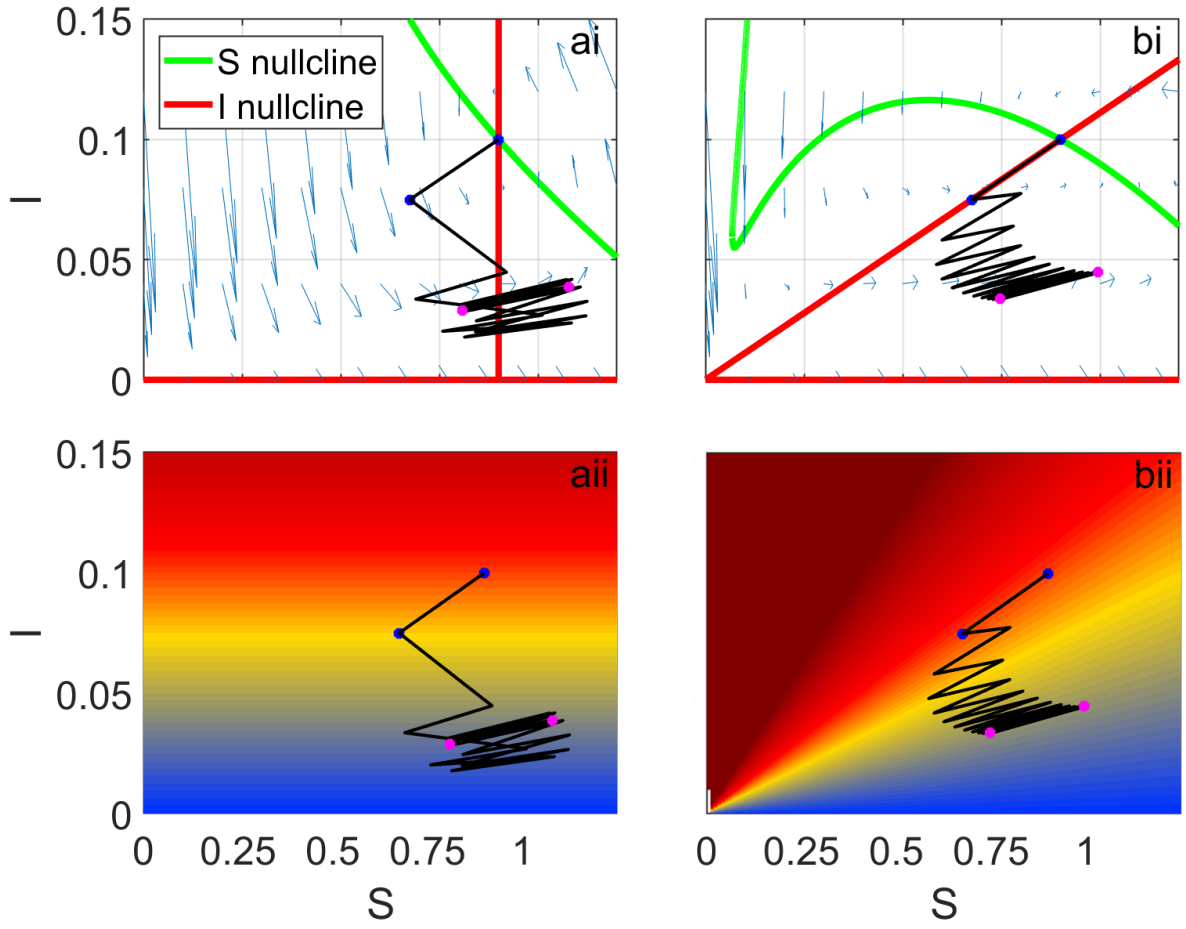

Figure 2: The population density response to repeated culling of 25% of the population for the SI model for (a) DD and (b) FD transmission. The figures show a population trajectory (solid black line) over the 30 cull events, with values immediately prior to and after the first cull highlighted with blue circles and before and after the 30th cull with magenta circles. In (i) the population trajectory is shown in phase space with the red lines showing the boundary between regions where I is decreasing and increasing; and the green lines show the boundary where S is decreasing and increasing (as indicated by the flux arrows in the figures). In (ii) the population trajectory is superimposed over the force of infection $\theta(I, N)$ with the colour changing from dark blue to dark red as the force of infection increases. Results are shown for a virulent infection, $\alpha = 4$, and with an initial endemic disease prevalence of $p_i = 10\%$. Parameters are as in figures 1a(ii) and 1b(ii) for DD and FD transmission respectively.

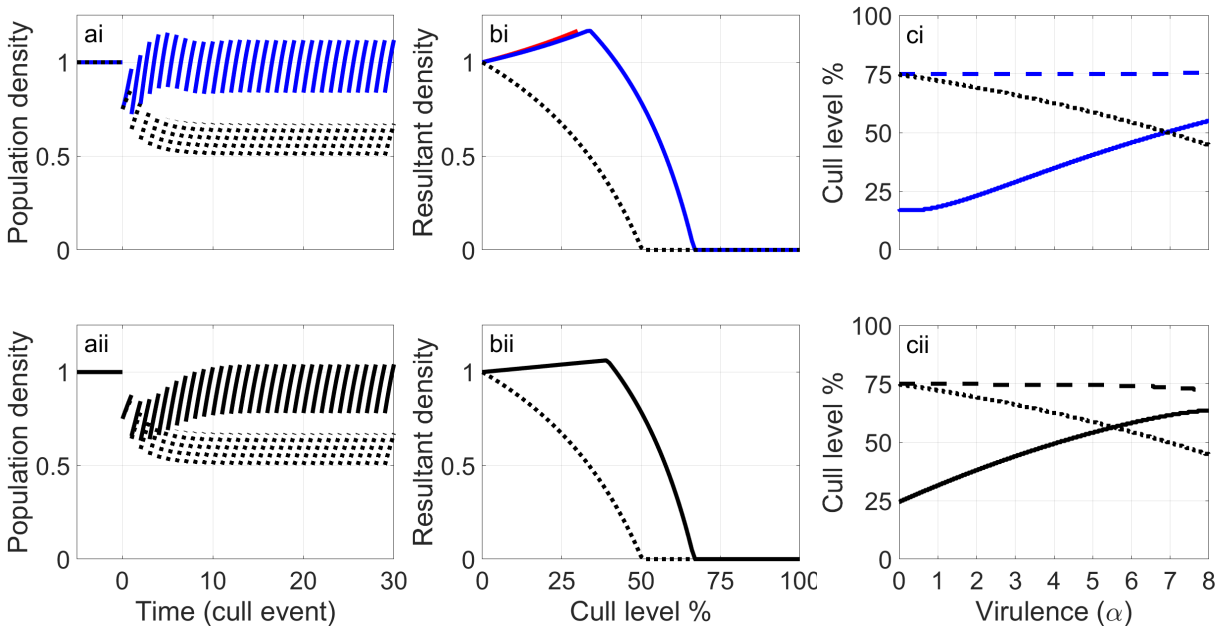

Figure 3: The population density compensatory response to culling for the SI model. (a) the population density response to repeated culling of 25% of the population for the full model, equations (1-3), under SI ($\gamma = 0$) dynamics for (i) DD transmission (blue) and (ii) FD transmission (black) and for the demographic effects only model (dotted). (b) the resultant population density at the end of sequential cull and subsequent regrowth periods for different levels of culling for the full model with (i) DD transmission (blue) and (ii) FD transmission (black), the demographic effects only model (dotted) and in b(i) the disease effects only model (red). Note this (red) line is only valid for culling levels less than 30% with higher culling levels leading to disease and population extinction. The difference between the solid blue and the dotted line (b(i)) and the difference between the solid black line and the dotted line (b(ii)) represent the amount of compensation due to the disease effects and in (b(i)) the difference between the red line and the blue line represents the compensation due to demographic effects. (c) plot of virulence against the level of culling required to eradicate the infection (solid line) and the population (dashed line) as well as the level of culling to eradicate the population in the demographic effects only model (dotted line) for (i) DD transmission and (ii) FD transmission. Results are shown for a virulent infection, $\alpha = 4$, (except in (c) where α varies) and with an initial endemic disease prevalence of $p_i = 10\%$. Other parameters are as in figure 1.

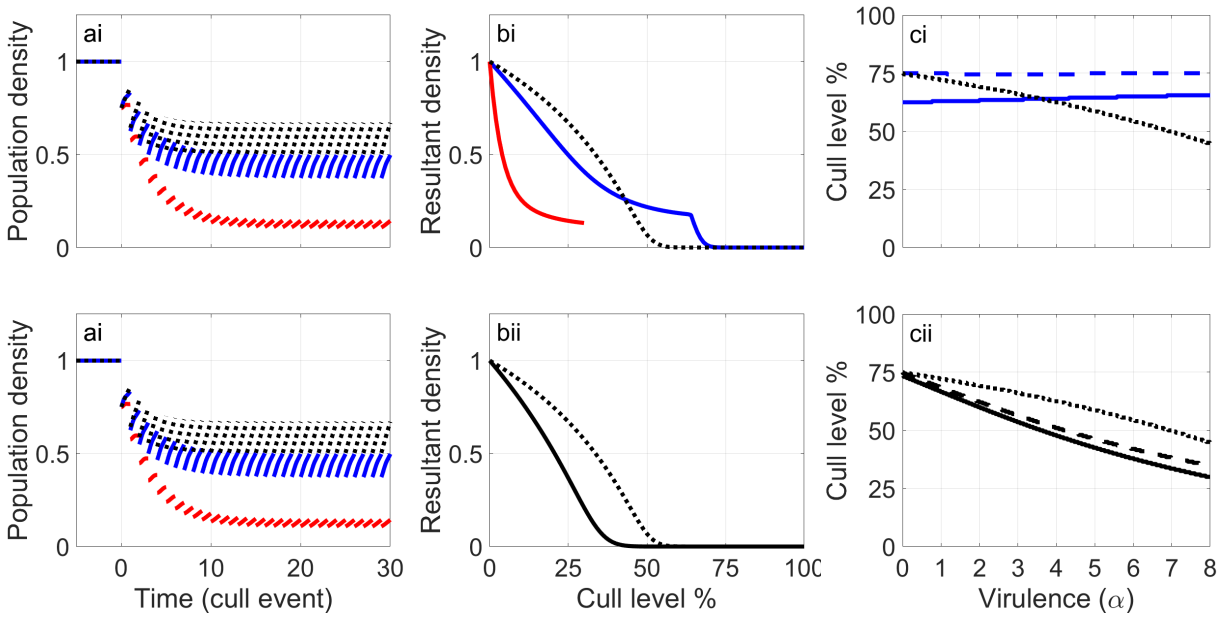

Figure 4: The population density compensatory response to culling for the SIR model. (a) the population density response to repeated culling of 25% of the population for the full model, equations (1-3), under SIR ($\gamma = 4$) dynamics for (i) DD transmission (blue) and (ii) FD transmission (black), for the demographic effects only model (dotted) and for the disease effects only model (red). Here the presence of the disease leads to a lower population in response to culling. (b) the resultant population density at the end of sequential cull and subsequent regrowth periods for different levels of culling the full model with (i) DD transmission (blue) and (ii) FD transmission (black), the demographic effects only model (dotted) and the disease effects only model (red). Note this (red) line is only valid for culling levels less than 30% with higher culling levels leading to disease and population extinction. The difference between the solid blue and the dotted line (b(i)) and the difference between the solid black line and the dotted line (b(ii)) represent the amount of compensation due to the disease effects and in (b(i)) the difference between the red line and the blue line represents the compensation due to demographic effects. (c) plot of virulence against the level of culling required to eradicate the infection (solid line) and the population (dashed line) as well as the level of culling to eradicate the population in the demographic effects only model (dotted line) for (i) DD transmission and (ii) FD transmission. Results are shown for a virulent infection, $\alpha = 4$, (except in (c) where α varies) and with an initial endemic disease prevalence of $p_i = 10\%$. Other parameters are as in figure 1.

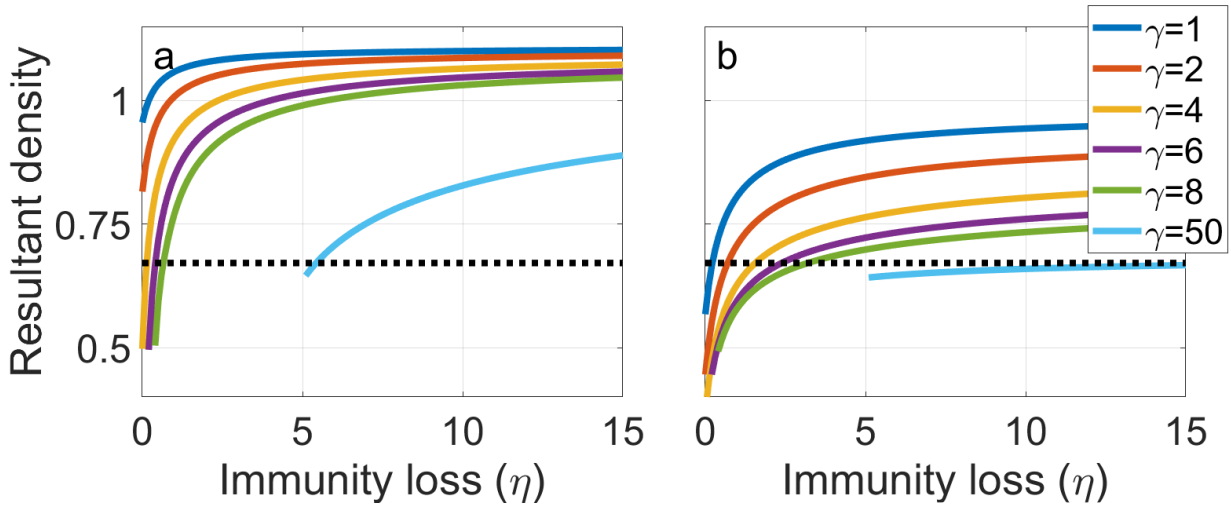

Figure 5: The resultant population density after 30 sequential cull and subsequent regrowth periods culling 25% of the population for the SIRS model (equations (1-3)) plotted against waning immunity, η, for different levels of recovery, γ, for (a) DD and (b) FD transmission. The dotted line represents the resultant population density for the demographic effects only model. The difference between the solid lines and dotted line represents the positive or negative compensatory effect due to changes in the disease dynamics. Results are shown for an initial endemic disease prevalence of $p_i = 10\%$. Other parameters are as in figure 1. Truncated results indicate parameter levels that do not satisfy requirements for valid solutions (equation (A8) & online appendix A, equation A9).

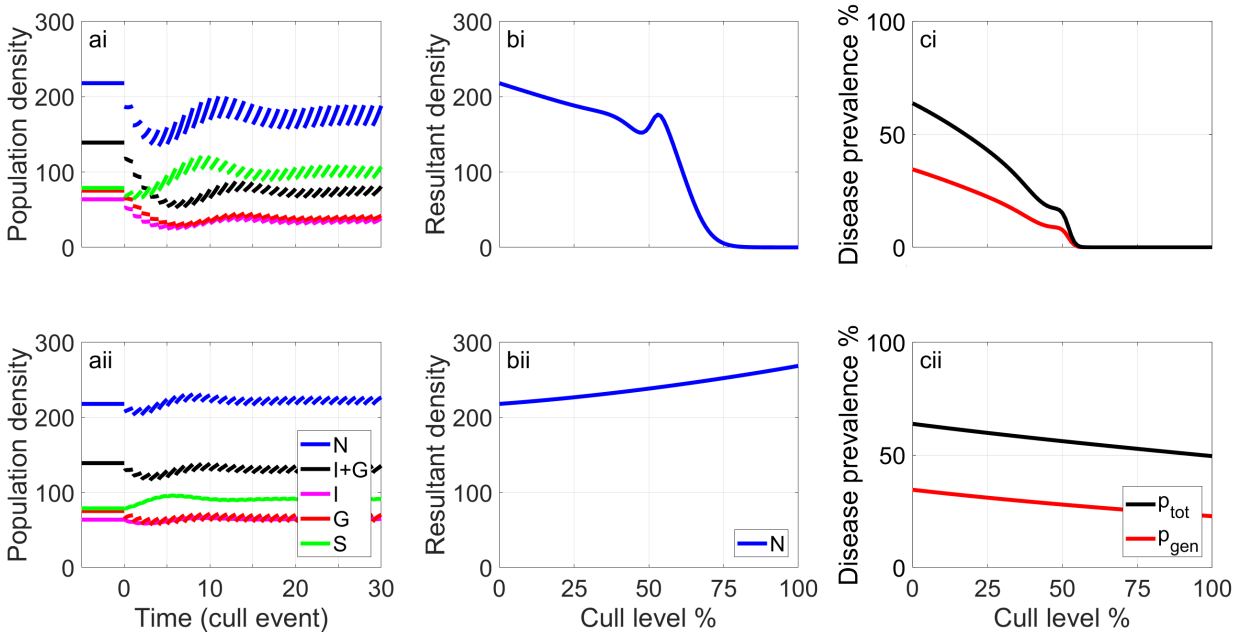

Figure 6: Results for the wild boar TB model in response to 30 cull events of 25% for (i) indiscriminate culling of the yearling and adult population and (ii) targeted culling of generalized yearlings and adults. The population dynamics over time are shown in (a) for total density (blue); infected and generalized density (black); infected density (magenta); generalized density (red) and susceptible density (green). The initial population assumes a TB prevalence, (I+G)/N, of 64% and a generalized prevalence, G/N, of 35%. (b) shows the resultant total population (blue) and (c) the total prevalence (black) and generalized prevalence (red) after 30 sequential cull and subsequent regrowth periods for different levels of hunting. The model and its parameters are outlined in A7.

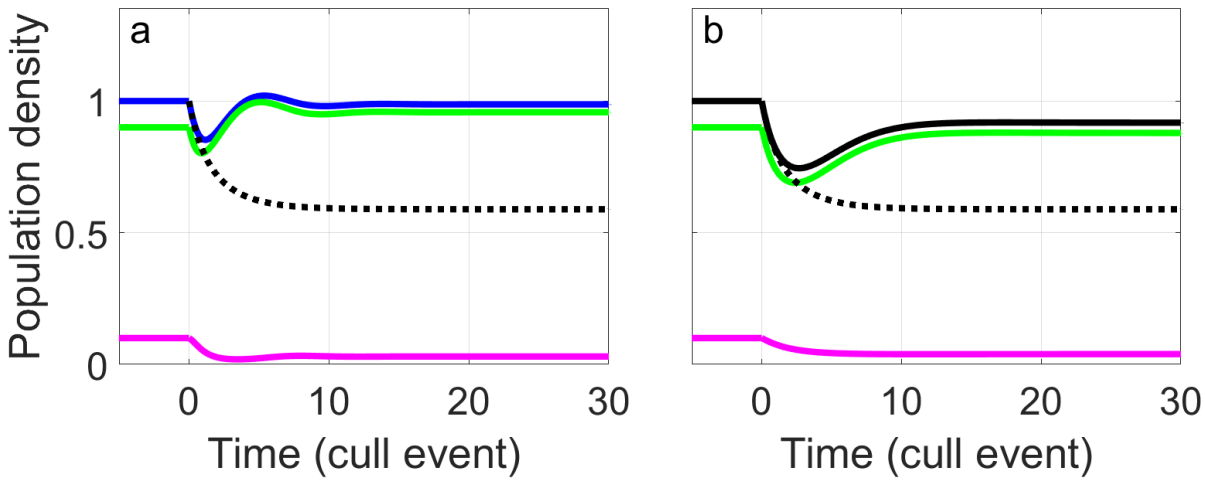

Figure A1: The population density response to continuous culling at rate $c = \log(1/(1-0.25))$ in an SI framework in equations (A10-A12) (here culling is at a similar rate to in the discrete culling model). The change in population density is shown for the total population density (blue for DD (a), black for FD (b)); the total density of susceptibles (green); the total density of infected (magenta) and the demographic effects only model (equation (A13)) with the same level of continuous culling (black dotted). (a) shows results for DD transmission and (b) shows results for FD transmission. Results are shown for a virulent infection, $\alpha = 4$, with no recovery to immunity ($\gamma = 0$), and an initial endemic disease prevalence of $p_i = 10\%$. Other parameters are as main paper, figure 1aii.

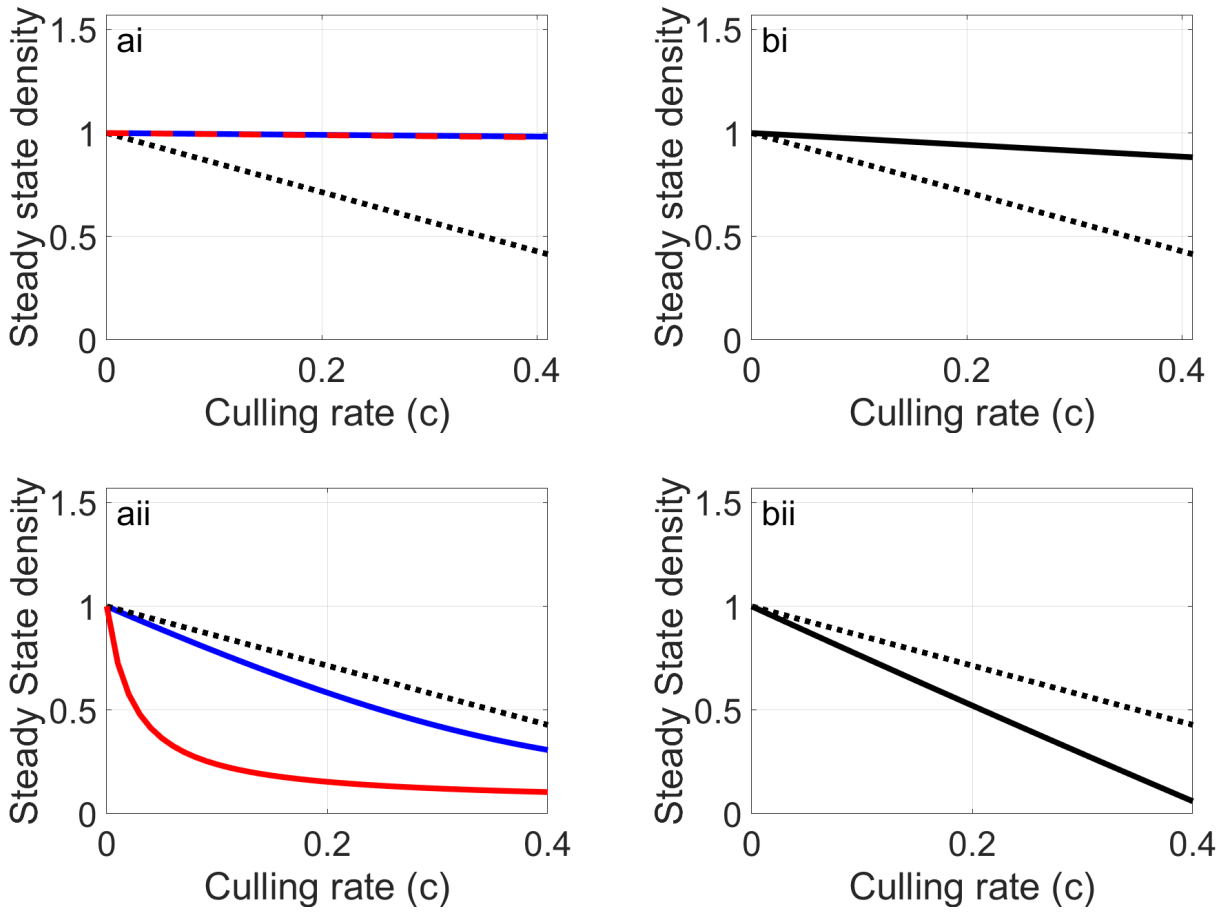

Figure A2: Results for the model with continous indiscriminate culling (equations (A10-A12) with $b(N) = b(1 - qN)$) for (i) the SI model and (ii) the SIR model. The steady state density N is shown for DD transmission in (a): for the full model (blue); the disease effects only model (red); and the demographic only model (black dotted). The steady state density N is shown for FD transmission in (c) for the full model (black) and demographic only model (black dotted). Other parameters are as in the main paper, figures 1ii & 1iv for the SI model and the SIR model respectively.

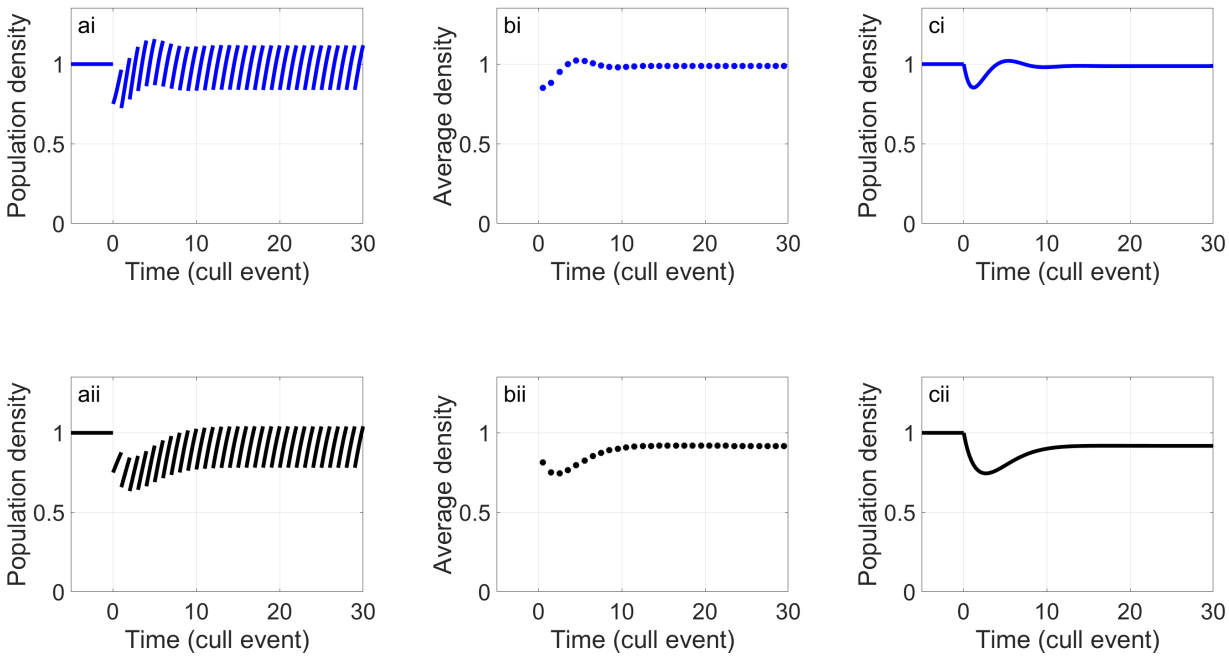

Figure A3: The population density response to culling for: (a),(b) a discrete annual cull of 25% and (c) continuous culling at rate $c = \log(1/(1-0.25))$ in an SI framework for (i) DD transmission and (ii) FD transmission. (a) shows the total population density during annual discreate culling, (b) shows the annual average total population density for the discrete cull, calculated by trapezium rule for the results obtained numerically over each regrowth period post the culling event. (c) shows the total population density under continuous culling. Other parameters are as main paper, figure 1a(ii).

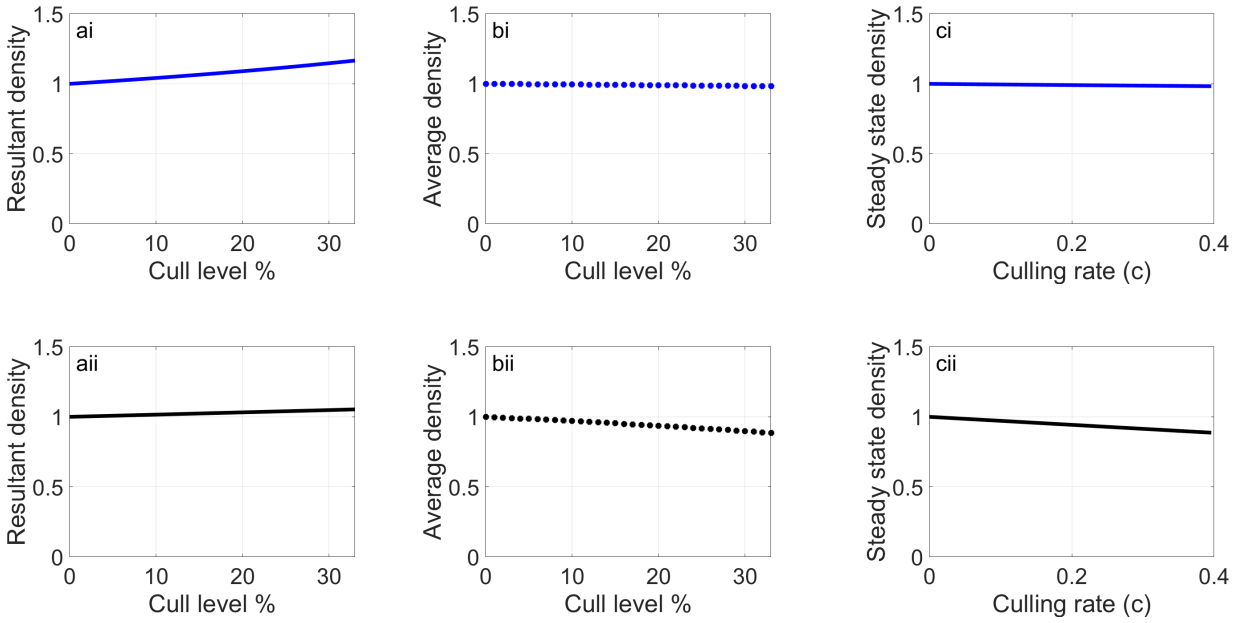

Figure A4: The population density response to culling for a range of culling levels in a SI framework for: (a),(b) a discrete annual cull and (c) continuous culling where culling rate $c = \log(1/(1-\delta))$ where δ is the equivalent discrete culling rate for (i) DD transmission and (ii) FD transmission. The change in population density is shown for the total population density (blue for DD (i), black for FD (ii)). (a) shows the resultant total population density after discrete annual culling and (b) shows the annual average total population density for the discrete cull, calculated by trapezium rule for the results obtained numerically over each regrowth period post the culling event. (c) shows the steady state total population density for the continuous culling model. Other parameters are as main paper, figure 1a(ii).

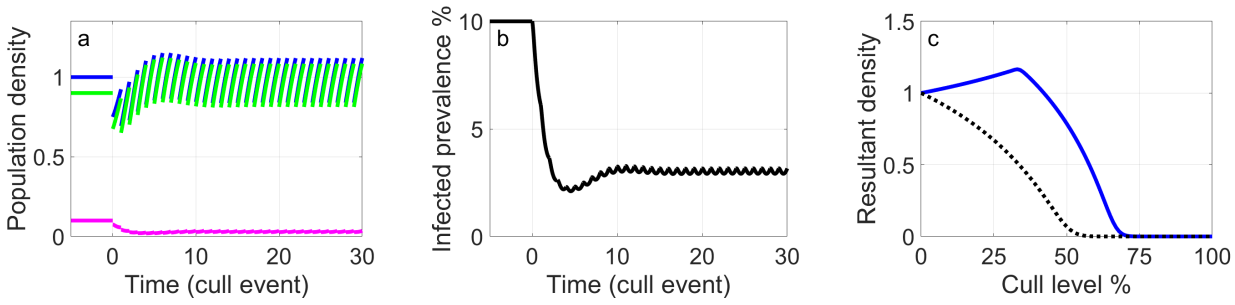

Figure A5: The population density and infected prevalence (I/N) response to culling in an SI framework with free-living transmission for equations (A44-A46). (a) shows the change in total population density (blue); the total density of susceptibles (green); and the total density of infected(magenta). (b) shows the change in disease prevalence over the cull events. (c) shows the resultant population density after 30 cull and subsequent regrowth events for different levels of culling for the free-living model (blue) and the demographic effects only model (equation (6)) (dotted). Results are shown for a virulent infection, $\alpha = 4$, and an initial endemic disease prevalence of $p_i = 10\%$. Free-living particles are excreted at rate $\lambda = 1$ and decay at rate $\mu = 6$. Other parameters are as main paper, figure 1a(ii).

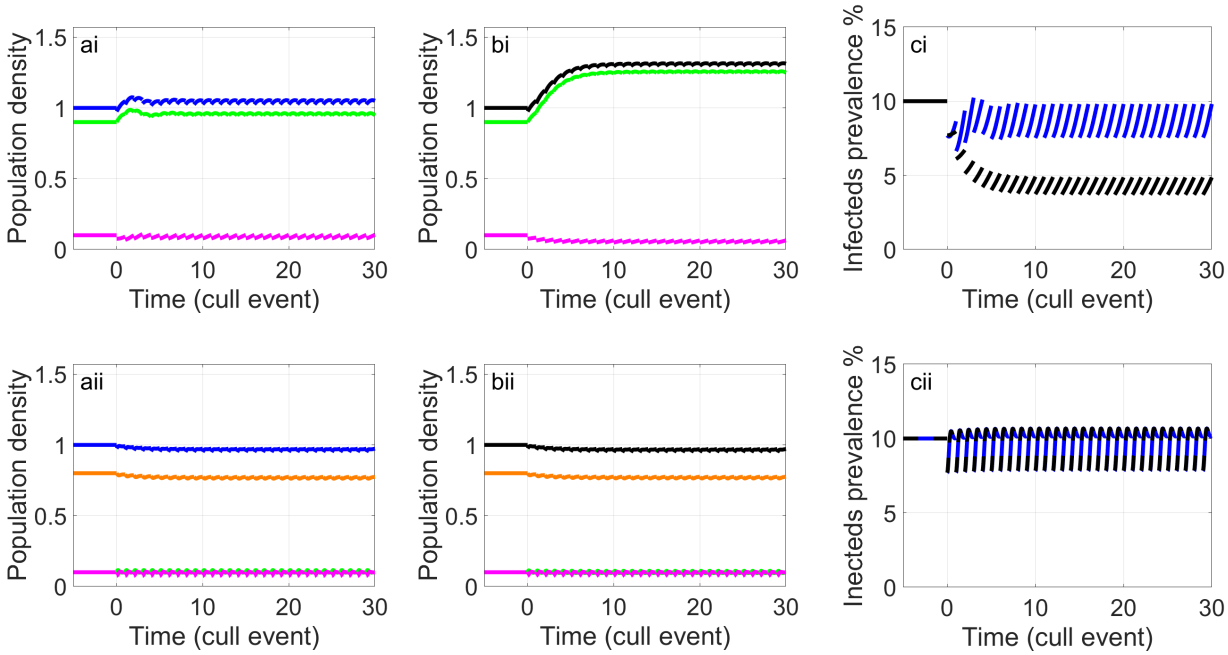

Figure A6: The population density and infected prevalence (I/N) response to targeted culling of 25% of infecteds only for equations (1-3). (i) shows results for the SI model, (ii) shows results for SIR model and (a) for DD transmission and (b) for FD transmission. Results show the total population density (blue for DD (a), black for FD (b)); the total density of susceptibles (green); the total density of infected (magenta); and the total density of recovered/immune (orange). (c) shows the disease prevalence for DD transmission (blue) and FD transmission (black), noting the prevalence response to culling is near identical for DD and FD transmission. Parameters are as in the main paper, figures 1ii & 1iv for the SI model and the SIR model respectively.

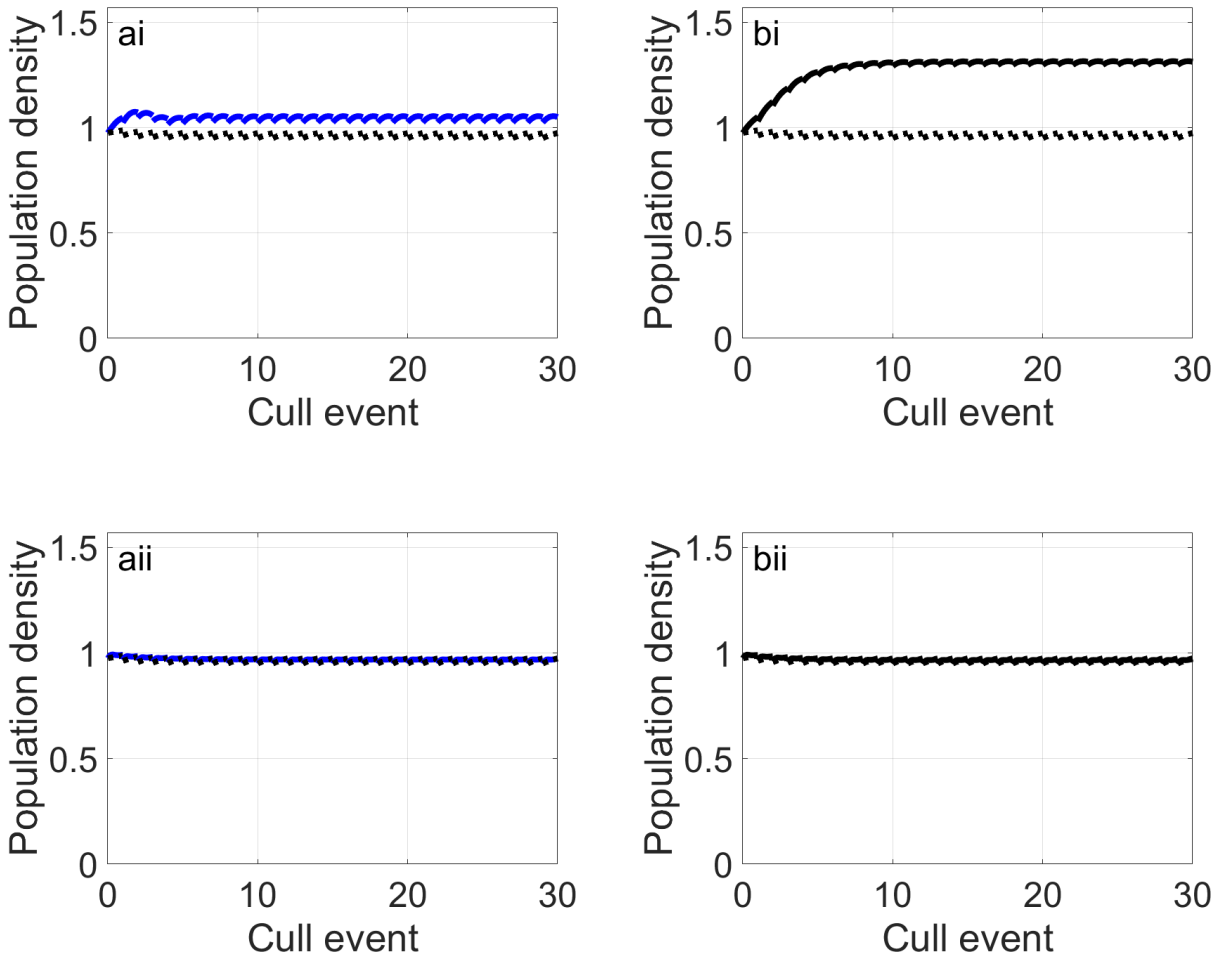

Figure A7: The resultant population density after 30 sequential discrete cull and subsequent regrowth periods for (i) the SI model and (ii) the SIR model for targeted culling 25% of infecteds only and an equivalent cull of $0.25 \times p_i$ in the demographic effects only model (equation (6)). (a) shows results for DD transmission (blue) and the demographic effects only model (black dotted) and (b) shows results for FD transmission (black) and the demographic effects only model (black dotted). Parameters are as in the main paper, figures 1ii & 1iv for the SI model and the SIR model respectively.

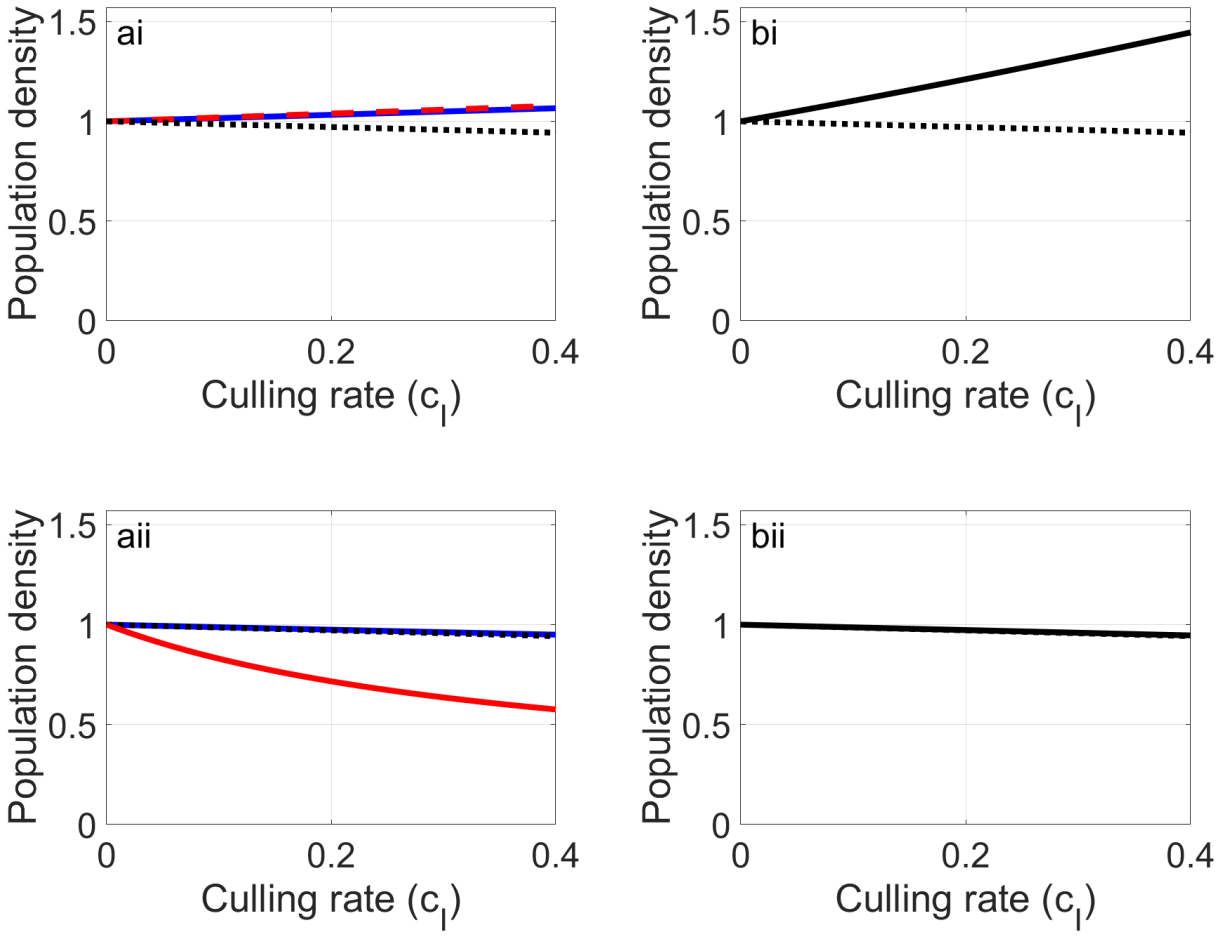

Figure A8: Results for the model with targeted infected cull level c_I for the continuous disease model (equations (A10-A12)) with $b(N) = b(1 - qN)$ for (i) the SI model and (ii) the SIR model. The steady state density N is shown for DD transmission in (a): for the full model (blue); the disease effects only model (red); and the demographic only model (black dotted). The steady state density N is shown for FD transmission in (b) for the full model (black) and demographic only model (black dotted). Parameters are as in the main paper, figures 1ii & 1iv for the SI model and the SIR model respectively.

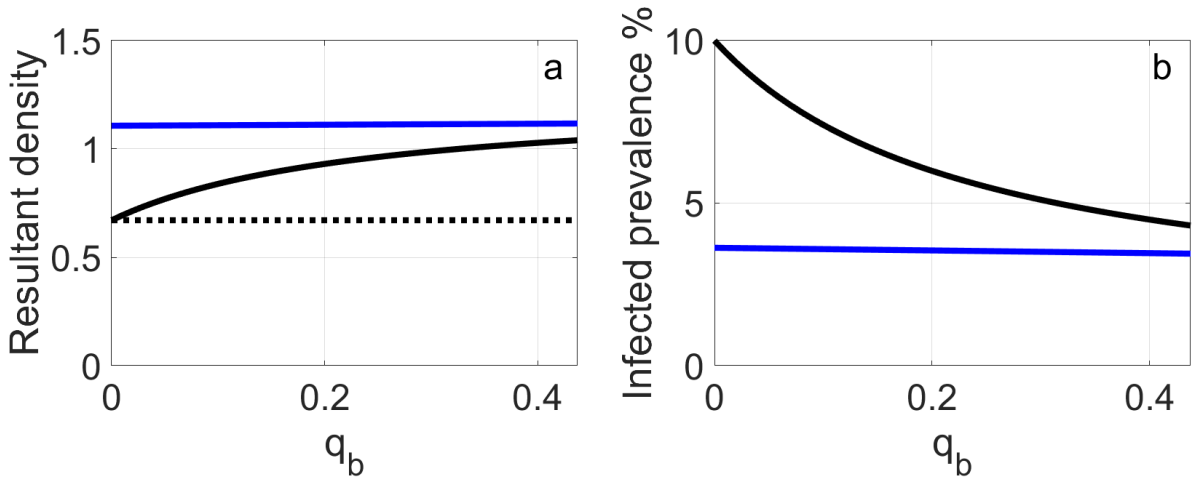

Figure A9: The resultant population density and infected prevalence (I/N) after 30 sequential cull and subsequent regrowth periods showing the response to 25% culling in an SI framework when varying q_b in equations (A64-A66). q_b runs from $q_b = 0$ representing density dependent death only to $q_b = (b - d - \alpha p_i)/(bN_e)$ representing density dependent birth only which is equivalent to the original model (SI framework equations (1-3)). (a) shows the resultant population density and (b) shows the change in infected prevalence as q_b varies for DD transmission (blue) FD transmission (black) and the demographic effects only model (equation (A71)) (black dotted). Results are shown for a virulent infection, $\alpha = 4$, and an initial endemic disease prevalence of $p_i = 10\%$. Other parameters are as main paper, figure 1a(ii).

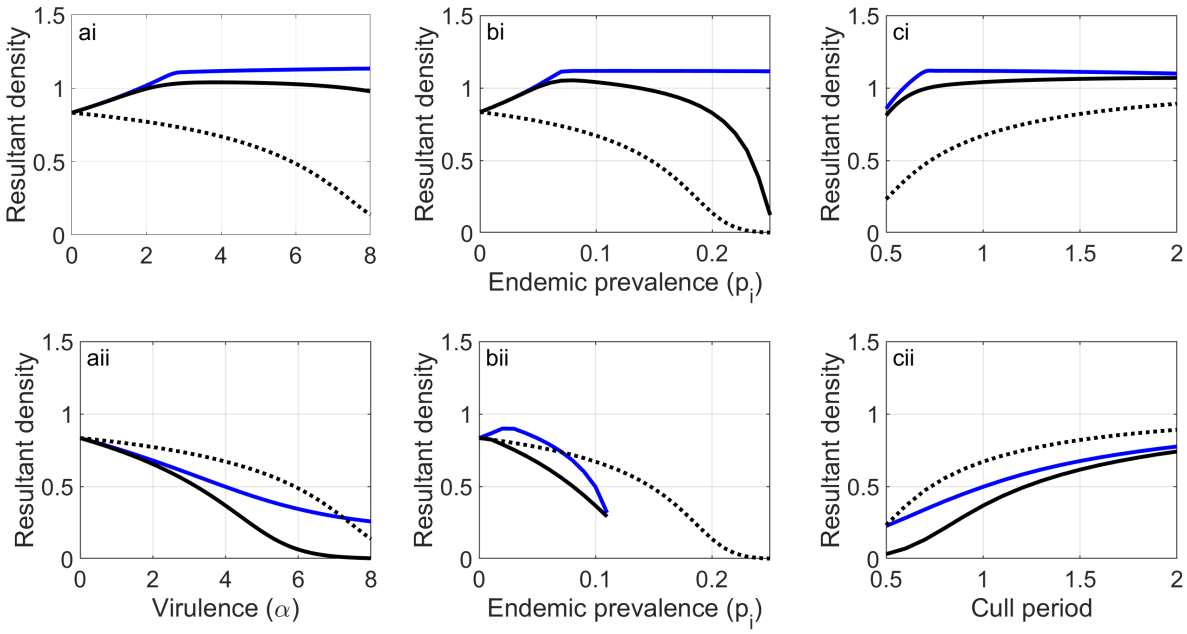

Figure A10: Parameter sensitivity for main paper equations (1-3). The resultant population density after 30 sequential cull (of 25% of the population) and subsequent regrowth periods for (i) the SI and (ii) the SIR model plotted against (a) virulence α, (b) initial endemic prevalence, p_i and (c) cull period (the time between sequential cull events) for DD transmission (blue), FD transmission (black) and the demographic effects only model (equation (6)) (dotted line). The difference between the solid lines and dotted line represents the positive or negative compensatory effect due to changes in the disease dynamics. When not varied in the figures the parameters are $\alpha = 4$, $p_i = 10\%$ and cull period = 1. Other parameters are as in the main paper, figures 1ii & 1iv for the SI model and the SIR model respectively. Truncated results (bii) indicate parameter levels that do not obey requirements for valid solutions (equations (A8) & (A9)).